



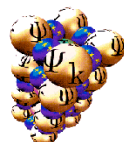
The Abdus Salam  
International Centre for Theoretical Physics



**SPRING COLLEGE ON COMPUTATIONAL NANOSCIENCE  
17 - 28 May 2010, ICTP, Trieste, Italy**

Co-sponsored by:

**CECAM, Psi-K NETWORK and DEMOCRITOS CNR-IOM**



Organizers:

**A. FOSTER, N. MARZARI and S. SCANDOLO**

**LIST OF  
POSTER PRESENTATION ABSTRACTS**



**SPRING COLLEGE ON COMPUTATIONAL NANOSCIENCE  
17 - 28 May 2010), ICTP, Trieste, Italy**

**Co-sponsored by:  
CECAM, Psi-K NETWORK and DEMOCRITOS CNR-IOM**

**LIST OF POSTER PRESENTERS (04.05.2010)**

**Lyudmyla ADAMSKA**

**Michele AMATO**

**Edgard P. M. AMORIM**

**Pedro A. S. AUTRETO**

**Jon Mikel AZPIROZ**

**Sananda BISWAS**

**Felipe CAMARGO DALMATTI ALVES LIMA**

**Hai Xia CAO**

**Prachi Avinash CHANDRACHUD**

**Hosein CHERAGHCHI**

**Gaston CORTHEY**

**R. FACCIO**

**Solange FAGAN**

**Xiaofeng FAN**

**Filippo L. FEDERICI CANOVA**

**M.Z.S. FLORES**

**Sriram GANESHAN**

**Rafael GONZALEZ HERNANDEZ**

**J. GULIN GONZALEZ (two posters)**

**Sanjeev Kumar GUPTA**

**Felix HANKE**

**M.J. HASHEMI**

**A.D. HERNANDEZ-NIEVES**

**Aaron HURLEY**

**M.V. KARACHEVTSEV**

**A. KASHYAP**

**Mohammad KHAZAEI**

**Sh. KHOSRAVIZADEH**

**Oleg O. KIT**

**S. KÖPPEN**

**Maricris LODRIGUITO MAYES**

**Monica MARINI**

**M. MAZZANI**

**Caetano R. MIRANDA**

**Mehdi NEEK-AMAL**

**Riku OJA**

**M. OZMAEIAN**

**Irina PETRESKA**

**Tanusri SAHA-DASGUPTA**

**K. SALORIUTTA**

**Julian SCHNEIDER**

**Giacomo SCIUTO**

**A.A. SHOKRI**

**P.L. TERESHCHUK**

**Mehmet TOPSAKAL**

**Mouna TRIKI EP SALLAMI**

**Madhvendra Nath TRIPATHI**

**M. ZARENIA**

**Martin E. ZOLOFF MICHOFF**

**Lyudmyla Adamska**

University of South Florida, Tampa, Florida

Research Poster***Rectification and stability of a single molecular diode***

L. Adamska, M. A. Kozhushner, I. Díez-Pérez, J. Hihath, Y. Lee, L. Yu, N. J. Tao, and I. I. Oleynik

In order to provide an insight to the nature of the rectification effect in chemically asymmetrical molecule [1], we performed first-principles calculations of atomic, electronic and transport properties of gold/molecule/gold junctions containing both symmetrical tetraphenyl and asymmetrical dipyrimidinyl-diphenyl diblock molecules. We found that in both molecules the charge transport occurs via hole resonant tunneling mechanism. The hole states are the charged states of the molecule. Therefore, the hole levels are raised or lowered in the external electric field approximately as  $\pm eV$  depending on the polarity of the applied bias  $V$ . In addition, the hole energy levels are renormalized by the image potential effects due to dispersive polarization interaction of the positive hole charge distribution over the molecule with the metallic electrodes. Such interaction is critically important to predict the correct value of the threshold turn-on voltage in current-voltage ( $I/V$ ) characteristics. The  $I/V$  curve for chemically-symmetric tetraphenyl molecule is symmetric, whereas dipyrimidinyl-diphenyl molecule displays asymmetric rectification behavior. Such effect is due to the strong asymmetrical localization of the hole ground state wave function in the external electric field and such an asymmetry in electronic structure is pinned by the underlying chemical differences between dipyrimidinyl and diphenyl blocks as the bias switched from positive to negative values.

## References:

1. I. Díez-Pérez, J. Hihath, Y. Lee, L. Yu, L. Adamska, M. A. Kozhushner, I. I. Oleynik, N. J. Tao, *Nature Chemistry* 1, 635 (2009)
2. L. Adamska, M. A. Kozhushner, I. I. Oleynik, *Phys. Rev. B* 81, 035404 (2010)

# Structural stability, electronic properties and quantum confinement effect in [110] SiGe nanowires

Michele Amato

*CNR-INFM-S<sup>3</sup> "nanoStructures and bioSystems at Surfaces", and Dipartimento di Fisica, Universita' di Modena e Reggio Emilia, via Campi 213/A, 41100 Modena, Italy*

Maurizia Palummo

*European Theoretical Spectroscopy Facility (ETSF), NAST, Dipartimento di Fisica, Università di Roma, 'Tor Vergata', via della Ricerca Scientifica 1, 00133 Roma, Italy*

Stefano Ossicini

*CNR-INFM-S<sup>3</sup> " nanoStructures and bioSystems at Surfaces", and Dipartimento di Scienze e Metodi dell Ingegneria, Universita' di Modena e Reggio Emilia, via Amendola 2 Pad. Morselli, I-42100 Reggio Emilia, Italy*

We report first principles calculations of [110] SiGe NWs; we discuss how the intrinsic bulk alloying effect and the extrinsic size effect have strong influence on their thermodynamic stability, on their electronic properties and on the nature of quantum confinement effect [1-3]. We analyze various types of SiGe NWs, which differ for the geometry of interface between Si and Ge. For each type of wire, we have analyzed how the variation of the composition and the diameter have a strong influence on the geometry of minimum energy, on the wave function localization and on the electronic band gap. Our study reveals that for SiGe NWs, unlike the corresponding pure NWs, the size, the geometry of SiGe interface and the composition have a primary role in the modulation of the structural and electronic properties.

- [1] M. Amato, M. Palummo, and S. Ossicini, Phys. Rev. B 80, 2355333 (2009)
- [2] M. Amato, M. Palummo, and S. Ossicini, Phys. Rev. B 79, 201302(R) (2009)
- [3] J. Yang, et al., Nano Lett. 6, 2679 (2006)

# Mechanochemistry in Cu nanowires: N and N<sub>2</sub> enhancing the atomic chain formation

E. P. M. Amorim and E. Z. da Silva

Instituto de Física “Gleb Wataghin”, UNICAMP,  
CP 6165, 13083-970, Campinas - SP, Brazil

We show using *ab-initio* total energy calculations based on density functional theory how H, B, C, O, S, N and N<sub>2</sub> impurities incorporated to copper nanowires obtained from previous tight-binding molecular dynamics calculations [1] and *ab-initio* calculations [2], could affect their electronic and structural properties. A novel mechanochemistry effect caused by N and N<sub>2</sub> when inserted in the linear atomic chain of copper nanowires was established. These impurities form not only stable but also very strong bonds, in such a way that they can extract atoms from a stable tip suggesting the possibility to produce longer atomic chains in a nitrogen atmosphere. This effect is caused by the formation of strong and stable p-d bonds in both cases. Besides our main result, we present a detailed discussion of the electronic structure for all impurities, also the forces and linear atomic chain distances before the rupture. The knowledge of these distances could be useful to explain larger distances between copper atoms that could be observed in High Resolution Transmission Electron Microscopy (HRTEM) images as well discussed in the literature for gold nanowires from the experimental [3, 4] and theoretical [5-7] point of views.

- [1] E. P. M. Amorim, A. J. R. da Silva, A. Fazzio, and E. Z. da Silva, *Nanotechnology* **18**, 145701 (2007).
- [2] E. P. M. Amorim and E. Z. da Silva, *Phys. Rev. B* **81**, 115463 (2010).
- [3] V. Rodrigues and D. Ugarte, *Phys. Rev. B* **63**, 073405 (2001).
- [4] W. H. A. Thijssen, D. Marjenburgh, R. H. Bremmer, and J. M. van Ruitenbeek, *Phys. Rev. Lett.* **96**, 026806 (2006).
- [5] F. D. Novaes, A. J. R. da Silva, E. Z. da Silva, and A. Fazzio, *Phys. Rev. Lett.* **90**, 036101 (2003).
- [6] N. V. Skorodumova and S. I. Simak, *Phys. Rev. B* **67**, 121404(R) (2003).
- [7] F. D. Novaes, A. J. R. da Silva, E. Z. da Silva, and A. Fazzio, *Phys. Rev. Lett.* **96**, 016104 (2006).

## The anomalous interatomic distances in Suspended Gold Atomic Chains

Pedro A.S. Autreto<sup>1</sup>, M.J. Lagos<sup>1,2</sup>, F. Sato<sup>3</sup>, V. Rodrigues<sup>1</sup>, D. Ugarte<sup>1</sup>, and D.S. Galvão<sup>1</sup>

<sup>1</sup>Institute of Physics “Gleb Wataghin”, University of Campinas - UNICAMP, 13083-970, Campinas, SP, Brazil.

<sup>2</sup>Brazilian Synchrotron Light Laboratory - LNLS, 13084-971, Campinas, SP, Brazil.

<sup>3</sup>Department of Physics, Federal University of Juiz de Fora - UFJF, 36036-330, Juiz de Fora, MG, Brazil.

The mechanical elongation of nanometric metal junction has attracted a great deal of interest from many researchers due to observation of very interesting physical phenomena associated to nanosystems, such as nanomechanics and conductance quantization, which must be studied for the practical implementation of nanotechnological devices. The stretching of gold point contacts has led to the discovery of the thinnest wire, a suspended linear atom chain (LAC). Since LAC discovery, different groups have reported interatomic distance between suspended Au atoms [1] that are much longer than in bulk gold. The observation of these long interatomic distances have been attributed to the existence of an impurity atom or molecule [2] inserted between two gold atoms, which are invisible in electron microscopy imaging due to its lower atomic number. In work we investigate the thermal effects and possible contaminant effects on the properties of suspended gold atomic chains using real-time atomic-resolution transmission electron microscopic (dynamical HRTEM) and the ab initio density functional total energy methods. By performing the experiments and theoretical study of LACs at different temperatures (150K and 300K), we have been able to get very precise information on the atomic species originating the anomalous long interatomic distances in gold LAC. Our results show an important difference between the histograms of bond length measurements in different temperatures. At low temperature, a wide peak centered about of 3 °Å dominates the histogram. This contrasts with the behavior of chains generated at 300 K, where two peaks coexist, (short 3.0 and long distances 3.6 °Å). The shorter distance population is attributed to clean gold-gold bonds, while the longer one is attributed to the presence of impurities. Our theoretical results have shown that water impurities yield a stable wire and, that the calculated Au-Au distances is 4.8 °Å independent of the temperature. So H<sub>2</sub>O may explain the very large distances (5 °Å) observed in the experimentally histograms. Concerning C and H impurities, predicted Au-Au distances are very similar (3.7 °Å) for both cases and, almost independent of temperature. We have also analyzed O and N impurities, where interatomic Au-Au correspond to values around 4 °Å. In this way, only C and H impurities yield distances in agreement with experimental results. To conclude which of these atoms could be presents in LAC, we have also analyzed the chemical nature of residual gases by mass spectrometry. Thought of this analysis and questioning how a LAC incorporates atomic of different species, we have been able to strong evidence that C atoms originated from the decomposition of adsorbed hydrocarbon molecules is more plausible impurity to explain the long metal-metal bond reported for Au LACs.

[1] H. Ohnishi, Y. Kondo, K. Takayanagi, Nature 395, 780 (1998).

[2] S.B. Legoas, D.S. Galvao, V. Rodrigues, D. Ugarte, PRL 88, 076105 (2002).

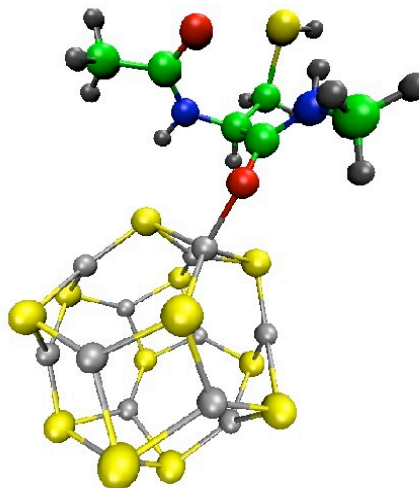
## ZnS NANOCCLUSERS IN BIOLOGICAL ENVIRONMENT. INTERACTION BETWEEN BARE AND ENDOHEDRALLY DOPED $Zn_{12}S_{12}$ NANOCCLUSERS AND L-CYSTEINE

Ion Mikel Azpiroz<sup>1</sup>

<sup>1</sup>Kimika Fakultatea, Euskal Herriko Unibertsitatea,  
PK 1072, 20080 Donostia, BASQUE COUNTRY (Spain)  
Tel. +34943015341, Fax +34943015270,  
Email : ionmikel.azpiroz@ehu.es

Understanding and controlling the organic-inorganic interface offers new paradigms in materials science, engineering, chemistry, biology and medicine.<sup>1</sup> In this sense, nanomaterials could be useful as biological probes for diagnosis and treatment of human diseases.<sup>2-4</sup> The purpose of the present theoretical work is to open a way to understand the behaviour of II-VI semiconductor hollow fullerene-like cluster in biological environment.<sup>5</sup> In particular, the interaction between a L-cysteine derived model and the  $Zn_{12}S_{12}$  cluster has been studied with the density functional theory (DFT). The L-cysteine model may interact in different ways with the Zn and S atoms of the nanocluster. Hence, multiple starting geometries for the complex formed by the L-cysteine model and the nanocluster have been considered. Geometry optimization and frequency calculations of such structures have been carried out in gas phase, and then single point calculations using the IEFPCM model have been performed at different dielectrics, in order to simulate the protein environment.

The results obtained suggest that the more stable complexes are the monodentate ones formed by binding carbonyl oxygen of the L-cysteine model and a Zn atom of the cluster, as may be seen in the attached figure. Different bidentate structures have been obtained too, where the bonding is between (1) the two oxygen atoms or (2) one of the oxygen atoms and the sulfur atom of the L-cysteine model and two atoms of Zn of the cluster. The interaction between L-cysteine model and endohedral  $X@Zn_{12}S_{12}$  has been studied too, being X Na or Cl. The first results show that Na and Cl doping stabilize binding from electronegative and electropositive atoms of the L-cysteine model, respectively.



<sup>1</sup> Sarikaya, M.; Tamerler, C.; Jen, A.; Schulten, K.; Baneyx, F. *Nat. Mater.* **2004**, *2*, 577.

<sup>2</sup> Whaley, S.; English, D.; Hu, E.; Barbara, P.; Belcher, A. *Nature* **2000**, *405*, 665.

<sup>3</sup> Lu, H.; Schoeps, O.; Woggon, U.; Niemeyer, C.M. *J. Am. Chem. Soc.* **2008**, *130*, 4180.

<sup>4</sup> Galian, R.E.; de la Guardia, M. *Trends in Analytical Chemistry* **2009**, *28(3)*, 279.

<sup>5</sup> Chung, S.Y.; Lee, S.; Liu, C.; Neuhauser, D. *J. Phys. Chem. B.* **2009**, *113(1)*, 292.

Adsorption of CO on graphene  
Sananda Biswas and Shobhana Narasimhan

Along with many other interesting applications, graphene has proved itself to be a promising candidate for gas sensing devices. The adsorbed molecule changes the carrier concentration of graphene one by one, thus leading to the step-like changes in resistance, which makes it possible to detect individual gas molecules adsorbed on graphene. Here we see how this is affected by the presence of defects on graphene.

We have studied mainly CO adsorption on defective graphene. Different defects like topological defect and vacancy defects has been studied using density functional theory calculations. We observed that the charge transfer between the graphene and the adsorbate depends on the type of graphene i.e, whether it is pristine or defective graphene. We noticed that higher the charge density of the C atom on the graphene sheet, higher the probability of adsorption of the adsorbate on the graphene.

## Computational investigation on the carbohydrate binding site of Frutalin

Filipe Camargo Dalmatti Alves Lima - fdlima@gmail.com - USP - São Paulo

Marcos Brown Gonçalves - browngon@if.usp.br - USP - São Paulo

Valtencir Zucolotto - zuco@ifsc.usp.br - USP - São Carlos

Helena Maria Petrilli - hmpetril@if.usp.br - USP - São Paulo

Frutalin is a tetrameric carbohydrate-binding protein obtained from breadfruit seeds [1]. Biomedical interest on frutalin comes from the high affinity exhibited by these molecules toward carbohydrates expressed by specific tumor cells[2]. So far, no theoretical computational studies have been carried out to investigate the binding characteristics of frutalin, which is probably due to the large number of atoms that should to be considered for *in silico* calculations. We investigate the binding of frutalin [1] with specific carbohydrate molecules [3] using a theoretical “cut-model”, considering only the carbohydrate binding site[4]. The spatial cuttings are performed with radius 4, 5 and 6 Å around the center of the carbohydrate ligand, including the aminoacids present in this region. We use the Carr-Parrinello Augmented Plane Wave (CP-PAW) method[5,6], which is an ab-initio all-electron reciprocal space method based on Kohn-Sham scheme of the density functional theory (DFT)[7]. The investigation of this very complex problem, can be divided into 3 main steps. In the first step, we study the electronic structure and structural properties of four isolated carbohydrates: A-D-Galactose, A-D-Mannose, A-D-Glucose and Lactose. In the second step, we study the isolated binding site of the protein and in a third step we investigate the interaction of the protein with each carbohydrate. Our theoretical results are compared with available measurements in each step. The study of the isolated carbohydrates allows us to demonstrate that our methodology is well suited to predict the electronic properties for carbohydrates since we found a very good agreement with experimental results[3]. Also our model for the protein is validated through comparison with UV spectroscopy and for this a semi-empirical theoretical calculation is done. The investigation of the third step is now in progress.

[1] P.T. Campana, Tese de Mestrado IFSC-USP (1998)

[2] V. Zucolotto, L.M. Beltramini F.C.D.A.Lima, H.M.Petrilli, Personal Communication (2009).

[3] <http://pubchem.ncbi.nlm.nih.gov/> (last access: 11/05/2009)

[4] A. Jeyaprakash, et. al. J. Mol. Biol. 347, 181 (2005).

[5] P.E. Blöchl, Phys Rev B., 50, 17953 (1994).

[6] R. Car, M. Parrinello, Phys RevLett. 55, 2471

[7] W. Kohn, L.J. Sham, PR 140, 1133 (1965).

# Magnetic and static nonlinear dielectric response in doped $\text{CdCr}_2\text{S}_4$

Hai-Xia Cao\* and Zhen-Ya Li

*Department of Physics and Jiangsu Key Laboratory of Thin Films, Soochow University, Suzhou,  
215006, China*

## **Abstract**

The influence of cation substitution on the magnetic and static nonlinear dielectric response in the doped magnetic relaxor ferroelectrics  $\text{CdCr}_2\text{S}_4$  is investigated within the framework of the spherical random-bond-random-field model (SRBRF) for the relaxor ferroelectric sublattice and the site-dilution Heisenberg model for the magnetic sublattice. In addition, an appropriate coupling term between the magnetic and ferroelectric subsystems has been taken into account. A-site substitution of the Cd by Fe in  $\text{Cd}_{1-x}\text{Fe}_x\text{Cr}_2\text{S}_4$  is found to reduce significantly the magnetization, which well agrees with the experimental results. Furthermore, the doping Fe ions play a crucial role in the spin-pair correlation and the nonlinear dielectric properties. It may provide an effective means to achieve the pronounced magnetoelectric coupling and the improved static nonlinear dielectric properties by substitution effect.

## **Acknowledgments**

This work was supported by the National Natural Science Foundation of China under Grant Nos. 10474069, 50832002 and 10904101, and the Natural Science Foundation of JiangSu Education Committee of China under Grant No. 08KJB140006.

---

\* Corresponding author. E-mail: [hxcao@suda.edu.cn](mailto:hxcao@suda.edu.cn)

## POSTER PRESENTATION

From graphene to *graphane* : A density functional investigation of metal insulator transition

The recent discovery of completely hydrogenated graphene, called as *graphane* has opened up new routes in the field of nanotechnology .Graphene is known to be a semi-metal with zero band gap while *graphane* turns out to be an insulator with band gap of 3.5eV (as calculated by DFT). The recent work on *graphane* shows that it is a promising candidate for hydrogen storage. In the present work we have probed the Metal-Insulator transition in graphene-*graphane* system within the framework of density functional theory. The primary aim of this work is understand how the band gap opens up. Therefore we have carried out electronic structure calculations for eighteen different hydrogen concentrations between graphene (0% coverage) and *graphane* ( 100% coverage) within the framework of DFT. For each concentration, the hydrogen atoms are placed contagiously, so as to form an island of hydrogenated carbon atoms. Such configuration is seen to be energetically lower than the random arrangement of the hydrogen atoms. We have analyzed the density of states (DOS) and iso-surfaces of the total charge density for each concentration and we summarise our findings as follows:

- For low concentrations, DOS resemble that of graphene.
- For higher concentration of hydrogen, say 30% and more, the region is dominated by finite DOS. The contribution at fermi level comes from the adjucent naked carbon atoms.
- Around 80%, since there are few naked carbon atoms to contribute, DOS approaches to zero with few mid gap states.
- The contribution to fermi level mainly comes from the delocalized  $p_z$  orbitals of the naked carbon atoms.
- The hydrogenated islands hardly contribute to the charge density giving rise to the insulating regions. These are surrounded by  $\pi$  bonded naked carbon atoms forming conducting regions.

Thus as the hydrogen coverage is increased, the semi-metal turns first into a metal, then transforms into an insulator. The metallic phase is spatially inhomogeneous in the sense, it contains the islands of insulating regions formed by hydrogenated carbon atoms and the metallic channels formed by contagious naked carbon atoms. Our investigations show that a specially designed partially hydrogenated graphene sheet could be a promising future material to be used for the purpose of devices.

# Nonlinear Electronic Transport through Zigzag Graphene Nanoribbons

Hossein Cheraghchi, Hanyeh Esmailzade

*Physics Department, Damghan University of Basic Sciences, Damghan, Iran*

## **Abstract:**

We investigate nonlinear transport through zigzag graphene nanoribbons (ZGNRs) with even and odd number of zigzag chains in width. For the case of odd and gated-even ZGNRs, a negative differential resistance (NDR) region with on-off ratio of the current up to  $10^7$  appears in the current-voltage characteristic curve. This NDR is originated to the selection rules based on parity conservation and also prohibition of transport between disconnecting energy bands. Our calculations based on non-equilibrium green's function formalism demonstrated that the details of the electrostatic potential profile along the ribbon can not affect the emerging of NDR in the I-V curve. Since external field is well screened close to the contacts, the electrostatic potential profile does not disturb the emerging of NDR phenomenon. However, in higher voltages than the NDR threshold voltage, due to charge transferring through the edges of ZGNR, screening would be so weak that the external potential penetrates inside the ribbon resulting in more reduction in the off-current. Furthermore, realistic ZGNRs may become asymmetric by the edge impurities and resulting in violation of the parity conservation. However, because of asymmetry-induced band gap appeared in the band structure of electrodes, the NDR phenomenon is preserved for some edge states.

## Investigating the Nature of Thiol Adsorption on Palladium: an Experimental and Theoretical Approach

Gastón Corthey<sup>a</sup>, Pilar Carro<sup>b</sup>, Aldo A. Rubert<sup>a</sup>, Guillermo A. Benitez<sup>a</sup>,  
Mariano H. Fonticelli<sup>a</sup> and Roberto C. Salvarezza<sup>a</sup>

a) Instituto de Investigaciones Fisicoquímicas Teóricas y Aplicadas (INIFTA), Universidad Nacional de La Plata - CONICET, Suc. 4 CC 16 (1900) La Plata, Argentina. E-mail: gcorthey@inifta.unlp.edu.ar  
b) Departamento de Química Física, Universidad de La Laguna, Tenerife, Spain

Self-assembled monolayers (SAMs) of alkanethiols on metals have attracted considerable attention because of the possibility to control the physical chemistry of surfaces at molecular level. This control has made possible several innovative applications ranging from molecular electronics to catalysis.<sup>1,2</sup> SAMs are easily formed by adsorption of thiols from solution. The self-assembly of alkanethiols on palladium is particularly interesting because the organic/metal interface formed involves a mixed layer containing both sulfides and thiols,<sup>3</sup> much more complex than the thiol/gold interface.

In this work, the composition and stability of alkanethiols adsorbed on palladium surfaces have been studied by electrochemical techniques, X-ray photoelectron spectroscopy (XPS) and density functional theory (DFT).

The adlayers have been prepared in liquid phase by immersion of the substrate in alkanethiols ethanolic solutions. Alkanethiols adsorbed on palladium surfaces lead to a complex interface composed of thiolate and sulfide, with surface coverage  $\theta_{\text{sulfide}} \approx 0.4$  and  $\theta_{\text{thiolate}} \approx 0.30$ , as observed from the XPS spectra and in accordance with previously reported results.<sup>2</sup> The adsorption of alkanethiols on a palladium adlayers, about 1.2 monolayers in thickness, deposited on Au(111) were also studied. These complex adlayers exhibit organic chainlength dependence barrier properties similar to those formed on gold and silver. On the other hand, these systems show an increased stability toward reductive desorption compared to alkanethiolate SAMs on silver and gold.<sup>4</sup>

Following the experimental data, we have performed a thermodynamic stability study of methanethiol and sulfide diluted layers on Pd(111), using density functional theory (DFT). We have found that as the chemical potential of the thiol in the gas phase is increased, the initially clean palladium surface is covered by a  $(\sqrt{3} \times \sqrt{3})R30$  sulfide lattice. Further increase in the pressure or concentration leads to the formation of  $(\sqrt{7} \times \sqrt{7})R19.1^\circ$  sulfide lattice that exhibits a short stability range because it undergoes a phase transition to form a complex  $(\sqrt{7} \times \sqrt{7})R19.1^\circ$  sulfide + thiol adlayer ( $3/7$  sulfur +  $2/7$  thiol coverage). This phase transition is accompanied by a strong surface reconstruction of the Pd(111) surface. This surface structure consists of sulfur atoms and thiol-Pd adatom-thiol units similar to those recently proposed for thiols on gold.<sup>5-8</sup> It is interesting to note that the chemical potential range to attain the  $(\sqrt{3} \times \sqrt{3})R30$  or the  $(\sqrt{7} \times \sqrt{7})R19.1^\circ$  sulfide lattices is not experimentally accessible. It means that these phases would only be observed if they were kinetically trapped, but not under equilibrium conditions.

- (1) Love, J.; Estroff, L.; Kriebel, J.; Nuzzo, R.; Whitesides, G. *Chem. Rev.* **2005**, *105*, 1103-1170.
- (2) Gates, B. D.; Xu, Q.; Stewart, M.; Ryan, D.; Willson, C. G.; Whitesides, G. M. *Chem. Rev.* **2005**, *105*, 1171-1196.
- (3) Love, J.; Wolfe, D.; Haasch, R.; Chabinyc, M.; Paul, K.; Whitesides, G.; Nuzzo, R. *J. Am. Chem. Soc.* **2003**, *125*, 2597-2609.
- (4) Corthey, G.; Rubert, A. A.; Benitez, G. A.; Fonticelli, M. H.; Salvarezza, R. C. *J. Phys. Chem. C* **2009**, *113*, 6735-6742.
- (5) Jadzinsky, P. D.; Calero, G.; Ackerson, C. J.; Bushnell, D. A.; Kornberg, R. D. *Science* **2007**, *318*, 430-433.
- (6) Walter, M.; Akola, J.; Lopez-Acevedo, O.; Jadzinsky, P. D.; Calero, G.; Ackerson, C. J.; Whetten, R. L.; Grönbeck, H.; Häkkinen, H. *Proc. Natl. Acad. Sci. U. S. A.* **2008**, *105*, 9157-9162.
- (7) Jiang, D.; Tiago, M. L.; Luo, W.; Dai, S. *J. Am. Chem. Soc.* **2008**, *130*, 2777-2779.
- (8) Li, Y.; Galli, G.; Gygi, F. *ACS Nano* **2008**, *2*, 1896-1902.

# Graphene & Graphene Nanoribbon: Electronic Structure and Mechanical Properties

**R. Faccio**, P. A. Denis, C. Goyenola, L. Fernández, H. Pardo & A. W. Mombrú

<sup>†</sup>*Cryssmat-Lab, DETEMA, Facultad de Química, Universidad de la República. Montevideo, Uruguay.*

## *Abstract*

Recently carbon-based materials have been the target of intensive research due to their possible technological applications and for its inherent biocompatibility. Here we will show an *ab initio* study of the induced magnetic moments in graphite creating single atom vacancies. In previous reports the appearance of magnetic moments was explained by the single presence of vacancies. In one hand, we will report how magnetic moment depends: position of vacancies, concentration and their alignment [1]. On the other hand we present the case of boron-doped graphene and boron-doped graphene with vacancies, discussing how magnetism depends on position of dopants [2], and its electronic structure.

Finally, pure zigzag graphene nanoribbon (GNR) terminated with hydrogen atoms shows localized states at edges. Here we will show its electronic structure and mechanical properties depend on the width of ribbons. These results indicates that GNR shows higher Young's modulus than graphene [3], and can be tuned adjusting its width.

## References

- [1] R. Faccio, H. Pardo, P. A. Denis, R. Yoshikawa Oeiras, F.M. Araújo-Moreira, M. Verissimo-Alves & A. W. Mombrú, *Phys. Rev. B* 77, 035416 (2008).
- [2] R. Faccio, L. Fernández-Werner, H. Pardo, C. Goyenola, O. N. Ventura & A. W. Mombrú. Submitted 2010.
- [3] R. Faccio, P. A. Denis, H. Pardo, C. Goyenola & A. W. Mombrú. *J. Phys.: Condens. Matter* 21, 285304 (2009). (Selected paper in IOP JPCM Highlights 2009)

## IRON- AND IRON OXIDE-FILLED SINGLE-WALLED CARBON NANOTUBES AS GAS SENSORS: A FIRST PRINCIPLE STUDY

*Solange B. Fagan, Rochele C. A. Bevilaqua, Ivana Zanella*

*Mestrado em Nanociências, Centro Universitário Franciscano – UNIFRA, Santa  
Maria – RS, Brazil*

The new materials research is the base of the technological development allowing improving the nature knowledge and its use in sustainable form. In this way, for an innovative technology, the carbon nanotubes (CNs) are distinguished [Iijima, 1991 Nature 356 56]. CNs had given a new breath to the technological research, extending possibilities of construction devices and equipment, even many times stimulated by the economic interest, but finally it brings improvements for the life quality of all. The CNs has been studied as potential materials for basic elements for nanoscales devices. They can be metals or semiconductors depending only on the geometric characteristics and thus they can be used in nanoelectronic devices, as well as in memory devices. The carbon tubes are materials with high susceptibility of mechanical tensions and a big surface to adsorbed atoms or molecules that can be used as biological and chemical sensors. However, the use of CNs in pristine form is not viable as gas sensors for very stable molecules due to the unfavorable adsorption. Consequently, a possible way to solve this problem is the use of functionalized CNs or some type of material that makes possible the association of these nanostructures with gases or other molecules [Fagan, 2003 Phys. Rev. B 67 033405]. In this way, this work present the electronic, magnetic and structural properties of the (8,0) single-walled carbon nanotubes (SWNTs) filled with iron and iron oxide submitted to the N<sub>2</sub> and O<sub>2</sub> adsorption. A recent experimental work [Cava, 2007 Chem. Phys. Letters 444 304-308] shows that the electrical properties of CNs filled with iron oxide change significantly the gas adsorption when exposed to different atmospheres compared with pristine CNs. However, the procedures involved on the gas adsorption are not clear yet. So, through first principles simulations it is possible to observe the iron and iron oxide filled SWNTs with O<sub>2</sub> e N<sub>2</sub> adsorption. For this study we use the density functional theory to describe the wave function for the atomic state and also using the pseudopotentials, basis set approximation, that are implemented on the SIESTA (Spanish Initiative for Electronic Simulations with Thousand of Atoms) code. In this way, it is possible to evaluate the band structures and binding energies of the semiconductors SWNTs pristine or filled when exposed to different atmospheres like O<sub>2</sub> e N<sub>2</sub> in order to evaluate the possibility for use them as gas sensors.

## **The weak interaction between finite carbon chains and single wall carbon nanotube**

X.F. Fan, L. Liu, J.L. Kuo and Z.X. Shen

*School of Physical and Mathematical Sciences, Nanyang Technological University, Singapore  
637616, Singapore*

With density-functional theoretical calculation, the structural, electronic and vibrational properties on the free finite carbon chains and those encapsulated inside carbon nanotubes (CNTs) are studied. The end effect and chain symmetry are found to play key roles in deciding the structural characteristics of the free finite carbon chains which rely on the parity of the number of carbon atoms. Due to the potential interaction between the carbon chains and CNTs, the electrons of the chain-CNT system will redistribute and some part of charge from CNT transfer to the inside carbon chain. We suggest that the attractive potential of chain atoms inside CNTs may be the driving force of formation for the linear carbon inside CNTs. It is also found that inside CNTs the carbon chains with even-number carbons present almost constant bond length alternation which is independent of the chain length. This trend of the even-number carbon chains in CNT helps to explain the universal experimental observation that the Raman peaks from chains in CNTs are within  $1820\text{-}1860\text{ cm}^{-1}$ .

## Role of the tip in NC-AFM energy dissipation

Filippo Federici Canova<sup>1</sup> and Adam S. Foster<sup>1,2</sup>

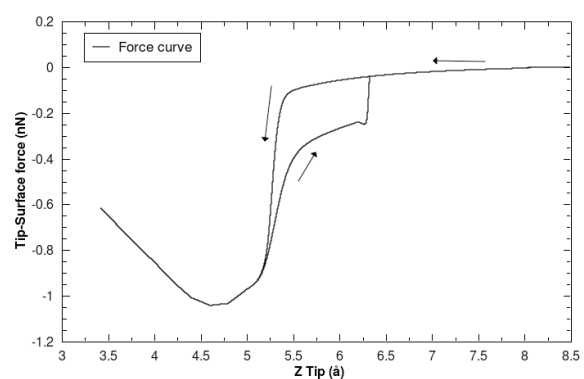
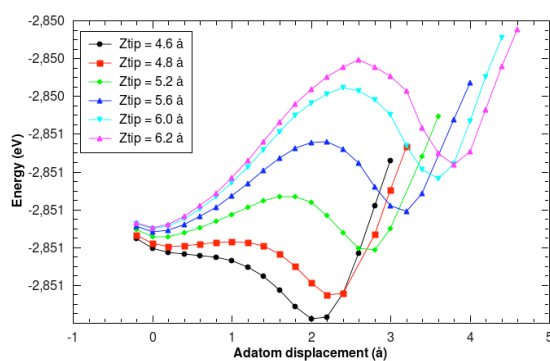
<sup>1</sup>Department of Physics, Tampere University of Technology, Tampere, Finland.

<sup>2</sup>Department of Applied Physics, Aalto University, Helsinki, Finland

filippo.federici@tut.fi

NC-AFM is an invaluable tool when probing surfaces, providing atomic resolution topography and detailed three-dimensional force maps. As the tip scans the surface, it is common practice to record the feedback gain signal associated to the energy dissipated in the oscillation cycles. This dissipation signal often differs significantly from conventional topography images, with dissipation showing different contrast patterns, periodicity and tip-surface distance dependence. Although many different surfaces have been studied with atomic resolution in both topography and dissipation, a routine interpretation of these measurements has yet to be found. A particular problem is to devolve the influence of the tip from observed images, and to really understand the atomic processes at the surface responsible for dissipate energy.

In order to understand better the role of the tip is measured dissipation, we carried out extensive atomistic calculations using a wide variety of different tip materials and structures, and a simple NaCl (100) surface. Implementing our home-built virtual AFM, we simulated dissipation imaging based on the “double-minimum” approximation [1]. Our calculations pointed out how ideal tips fail to give dissipation, as they are too stable to generate any atomic reconstruction, while non-ideal, defected tips allow the system to hop between two metastable configurations as the tip approaches and retracts. The statistical hysteresis in the configurations probabilities ultimately cause an hysteresis loop in the force acting on the tip, giving energy dissipation of the same order of experimental data. Alongside static dissipation simulations, we also explore fully dynamic approaches taking advantage a recent development in computational architecture.



[1] L.N. Kantorovich and T. Trevethan, *Phys. Rev. Lett.* **93**, 236102 (2004)

## A Molecular Dynamics Study on the Formation of Graphane from Graphene Hydrogenation

M. Z. S. Flores<sup>1</sup>, P. A. S. Autreto<sup>1</sup>, S. B. Legoas<sup>2</sup> and D. S. Galvão<sup>1</sup>

<sup>1</sup>Applied Physics, State University of Campinas, Campinas, São Paulo, Brazil

<sup>2</sup>Centro de Ciências e Tecnologia, Federal University of Roraima, Boa Vista, Roraima, Brazil.

Recently, Elias *et. al.* [1] performed a series of elegant experiments which resulted on the formation of graphane from the well known two dimensional graphene under cold plasma exposure. These experiments proved the existence of a fully hydrogenated graphene, which was previously reported from Density Functional Theory calculations [2]. Graphane is a two-dimensional system consisting of a single layer of fully saturated ( $sp^3$  hybridization) carbon atoms. In an ideal graphane structure C–H bonds exhibit an alternating pattern (up and down with relation to the plane defined by the carbon atoms). Although both works were performed for the same system, their results didn't agree in all aspects, specially in relation to the graphane lattice parameter. This is due to a competition between the increase in the bond length and the tetrahedral nature of  $sp^3$  hybridization in carbon atoms, which lead to out of plane carbon in graphane. In this work we have investigated, using *ab initio* and reactive molecular dynamics simulations [3], the role of H frustration (breaking the H atoms' up and down alternating pattern) in graphane-like structures. Such frustrations include extra competition on lattice parameter determination regarding the presence of graphene, chairlike (hydrogen atoms alternating on both sides of the plane) and boatlike (hydrogen alternating in pairs) graphane domains [4]. Our results show that a significant percentage of uncorrelated H frustrated domains are formed in the early stages of the hydrogenation process leading to membrane shrinkage and extensive membrane corrugations. These results also suggest that large domains of perfect graphane-like structures are unlikely to be formed, as H frustrated domains are always present. The number of these domains seems to be sensitive to small variations of temperatures and H gas densities. This can perhaps explain the significant broad lattice parameter distribution values experimentally observed [1].

[1] D. C. Elias *et. al.*, Science 323, 610 (2009); arXiv:08104706.

[2] J. O. Sofo, A. S. Chaudhari, and G. D. Baker, Phys. Rev. B 75, 153401 (2007); arXiv:cond-mat/0606704.

[3] A. C. T. van Duin, S. Dasgupta, F. Lorant, and W. A. Goddard III, J. Phys. Chem. A 105, 9396 (2001).

[4] M. Z. S. Flores, P. A. S. Autreto, S. B. Legoas and D. S. Galvao, Nanotechnology 20, 465704 (2009); arXiv:cond-mat/0903.0278v1.

# The role of hydrogen bonding in water-metal interactions

(Stony Brook University)

January 30, 2010

The hydrogen bond interaction between water molecules adsorbed on a Pd-111 surface, a well known nucleator of two dimensional bilayers of ice at low temperatures, is studied using density functional theory calculations. The role of the exchange and correlation potential in the characterization of both the hydrogen bond and the water-metal interaction is analyzed in detail. We conclude that the choice of this potential is critical in determining the cohesive energy of water-metal complexes. The crucial factor nonetheless is not the description of the metal screening, even if this screening represents an important ingredient for the water-metal interaction. The different characterization of the hydrogen bonds between water molecules and the ( pseudo hydrogen bonds) established between the water and the surface is at the heart of the large disparity we observe in our calculations. These results put in evidence the urgent need for an accurate characterization of the hydrogen bond interaction with density functional theory.

## **Adsorption and incorporation of vanadium at the GaN(0001) surface.**

*Rafael González-Hernández and, Jairo Arbey Rodriguez*

*GEMA - Grupo de Estudio de Materiales. Departamento de Física, Universidad Nacional de Colombia. Bogota - Colombia*

We have carried out first-principles spin polarized calculations in order to study the energetics and electronic structure of vanadium adsorption and incorporation on GaN(0001)-2x2 surface using density functional theory (DFT) within a plane-wave ultrasoft pseudopotential scheme [1]. It was found that V atoms preferentially adsorb at the  $T_4$  sites at low and high coverages (from 1/4 up to 1 monolayer). In addition, calculating the relative surface energy of several configurations and various V concentrations, we constructed a phase diagram showing the energetically most stable surfaces as a function of the Ga chemical potential. Based on these results, we found that incorporation of V adatoms in the Ga-substitutional site is energetically more favorable compared with the adsorption on the top layers. Our calculations show that the vanadium incorporation is most favorable under a nitrogen environment, in agreement with recent experimental results.

[1] P. Giannozzi, S. Baroni, N. Bonini, M. Calandra, R. Car, C. Cavazzoni, D. Ceresoli, G. L. Chiarotti, M. Cococcioni, I. Dabo, *et al.*, Journal of Physics: Condensed Matter 21, 395502 (2009), URL <http://www.quantum-espresso.org>

# The behaviour of water confined in zeolites: molecular dynamics simulations vs. experiment

P Demontis<sup>1</sup>, J Gulín-González<sup>2</sup>, M Masia<sup>1</sup>  
and G B Suffritti<sup>1</sup>

<sup>1</sup> Dipartimento di Chimica, Università di Sassari and INSTM, Unità di ricerca di Sassari, Via Vienna 2, I-07100 Sassari, Italy

<sup>2</sup> Instituto Superior Politécnico José A. Echeverría (ISPJAE), Dpto. de Física, Marianao, La Habana, Cuba and Grupo de Matemática y Física Computacionales, Universidad de las Ciencias Informáticas(UCI), Carretera a San Antonio de los Baños, Km 21/2, Torrens, La Habana, Cuba

**E-mail:** gulinj@uci.cu

## Abstract

In order to study the behaviour of water adsorbed in zeolites, which are microporous crystalline aluminosilicates, whose channels and cavities of nanometric dimensions can host many different molecules, we developed a sophisticated empirical potential for water, including the full flexibility of the molecule and the correct response to the electric field generated by the cations and by the charged atoms of the aluminosilicate framework. The use of an empirical potential was needed because first principles molecular dynamics is not yet applicable to follow for nanoseconds the time evolution of several hundreds of atoms, as it is needed for the study of water adsorbed in zeolites. However, in the few cases where the comparison is possible, we have shown that the reproduction of experimental data by our potential model is similar or even better than that obtained from the first principles methods. The results (some of them still unpublished) of molecular dynamics simulations of water confined in a large variety of zeolites (one-dimensional chains in Li-ABW and bikitaite, nano-helices in natrolite, worm-like clusters in silicalite, spherical nano-clusters in zeolite A and ice-like nanotubes in AlPO<sub>4</sub>-5 and SSZ-24) at different temperatures and coverage (*loading*) are reviewed and discussed in connection with the experimental data, whose overall good reproduction encourages to attempt an atomic-scale description of structural and dynamical phenomena occurring in confined water. The results are also compared with simulations and experimental data of bulk water.

# The pressure-induced reversible amorphization of LTA zeolites. A study *via* energy minimization technique

J. Gulín González<sup>1\*</sup>, A. Dorta-Urra<sup>1</sup>, P. Demontis<sup>2</sup>, G.B. Suffritti<sup>2</sup>

<sup>1</sup> Instituto Superior Politécnico José A. Echeverría (ISPJAE), Dpto. de Física, Marianao, La Habana, Cuba Grupo de Física y Matemática Computacionales (GFMC), Universidad de las Ciencias Informáticas (UCI), Carretera a San Antonio de los Baños, Km 2½, Torrens, Boyeros, La Habana, Cuba.

<sup>2</sup> Dipartimento di Chimica, Università di Sassari and Consorzio Interuniversitario Nazionale per la Scienza e Tecnologia dei Materiali (INSTM), Unità di ricerca di Sassari, Via Vienna 2, I-07100 Sassari, Italy

\* *E-mail address:* [gulinj@uci.cu](mailto:gulinj@uci.cu)

## Abstract

A previous computational study on dehydrated LTA zeolites suggested the reversible amorphization of calcined LTA samples at pressures below 6 GPa, in agreement with experimental results. However, the effect of guest molecules on the amorphization process was not evaluated in that study. In the present paper, the potential reversible amorphization of Xe containing LTA samples under high external pressures is studied *via* energy minimization calculations. The results of the simulations confirmed the pressure-induced amorphization of LTA zeolites at pressures about 2-4 GPa for all the studied samples. Besides, the simulations stressed the importance of the structural topology, particularly of D4R secondary units, for the recovering of the crystalline order. According to our calculations the exchangeable cations (Na<sup>+</sup> and Li<sup>+</sup>) play a crucial role in the process of amorphization. Our results suggest that the reversible amorphization is essentially independent on the presence of Xe molecules in the range of the pressures studied (6 GPa).

**Keywords:** Microporous Materials; LTA zeolites; Crystal Structure; Phase Transitions; Pressure-Induced Amorphization

# Density functional calculation of the phonon properties in the III (Ti, V, Cr)-nitrides crystals

Sanjeev K. Gupta, Sanjay D. Gupta, Prafulla K. Jha and Sankar P. Sanyal<sup>#</sup>

*Department of Physics, Bhavnagar University, Bhavnagar, 364 022, India*

*<sup>#</sup>Department of Physics, Barkatullah University, Bhopal, 462 026, India*

**Abstract:** Density functional calculation is employed to calculate the phonon properties of 3d metal (Ti, V, Cr) nitrides. The results are given for lattice constant, charge density, band structure and phonon properties and electron-phonon interaction coefficient. The results agree well with the available experimental and other reported data.

The III-nitride compounds have deserved great experimental and theoretical attention in connection with their potential applications in optoelectronics and spintronics [1-2]. They are characterized by hardness, high melting point, which class them among the refractory compound, excellent electrical and thermal conductivity, high chemical and thermal stability and good wear and corrosion resistance. Chromium nitride (CrN) is produced recently, and there are controversies concerning its lattice structure, elastic properties and phonon properties particularly for phonon dispersion curves [3, 4]. Inelastic-neutron-scattering measurements [5] revealed that the acoustic branches of the phonon spectrum of rocksalt VN are completely different compared to TiN and CrN, and the anomalies of the phonon spectra are shifted to the X-point of the Brillouin zone (BZ), while for other metal nitrides (CrN and TiN) with B1 structure the special features of the phonon spectra are located near the high symmetry directions. Isaev *et al* [3] reported imaginary phonon frequencies along the high symmetry  $\Gamma$ -X direction of the phonon dispersion curve for VN, which reflects that the structure is other than rocksalt, motivated us for the present study of VN. In the present work, we have carried out a systematic *ab initio* calculation of phonon properties for the rocksalt phase for TiN and CrN and zinc-blende (ZB) and rocksalt phases for VN to settle down the controversies on structural and vibrational properties for these metal nitrides [2-4].

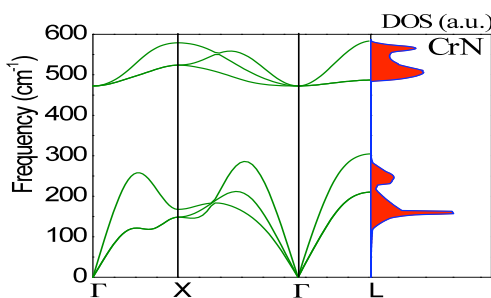


**Fig. 1:** Phonon-dispersion curves along high symmetry direction and phonon density of states (PDOS) for CrN rocksalt crystal.

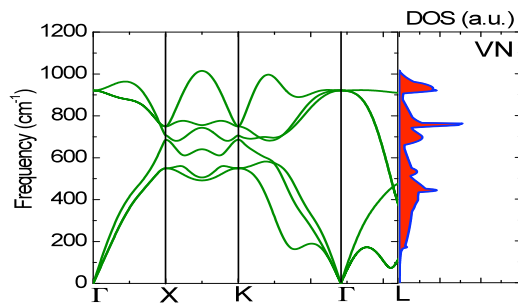


**Fig. 2:** Phonon-dispersion curves along high symmetry direction and phonon density of states (PDOS) for VN zinc-blende crystal.

We have used the pseudopotential planwaves method within generalized gradient approximation (GGA). The optimized structural and vibrational parameters are obtained from our studies using PWSCF code [6]. The Fig. 1 and Fig. 2 present the phonon dispersion curve and phonon density of states for rocksalt CrN and ZB-VN respectively. Acoustic and optical branches are separated by a frequency gap of around  $200 \text{ cm}^{-1}$  for CrN and TiN, which increases as the period number is increased and mass ratio decreased. In contrast to CrN, the acoustical branches of VN show anomalies in K- $\Gamma$ -L direction. The electron-phonon coupling coefficient is in the range of 0.59-0.67 for nitride (Ti, V and Cr) systems.

[1] E. L. Toth, Transition Metal Carbides and Nitrides, Academic Press, New York, 1971.

[2] R.-de Paiva, R. A. Nogueira, J. L. Alves, *Phys. Rev. B* **75**, 085105-085116 (2007) and references there in.

[3] E. I. Isaev *et al*, *J. Appl. Phys.* **101**, 123519-123537 (2007) and references there in.

[4] A. Filippetti, W. E. Pickett and B. M. Klein, *Phys. Rev. B* **59**, 7043-7050 (1999).

[5] W. Weber, P. Rödhammer, L. Pintschovius, W. Reichardt, F. Gompf and A. N. Christensen, *Phys. Rev. Lett.* **43**, 868-871 (1979).

[6] S. Baroni, A Corso Dal, S. de Gironcoli and P. Giannozzi, <http://www.pwscf.org>.

# Theoretical investigation of the switching mechanism in a single-molecule memory unit

Felix Hanke & Mats Persson

Surface Science Research Centre, University of Liverpool, Liverpool, UK

The storage and retrieval of information at the sub-nanometer scale is one of the outstanding challenges in nanoelectronics. It was recently proposed that the molecular switch naphthalocyanine can be controlled using scanning-tunneling microscopy (STM) [1] when it is adsorbed on a thin layer of NaCl. The on/off state of naphthalocyanine is determined by the orientation of two central hydrogen atoms, which changes with the application of a high STM voltage, while a low voltage allows to read out the molecular state. Despite the wealth of available experimental information, the electronic processes responsible for the STM-induced configurational changes in naphthalocyanine are poorly understood theoretically.

This project aims to explain the switching property based on density functional theory. Naphthalocyanine is studied both in vacuum and adsorbed on a NaCl surface. According to our calculations, there are two equivalent adsorption sites. From both adsorption geometries on the NaCl surface as well as in vacuum, the reaction path for the hydrogen switching is computed. The switching in vacuum proceeds in two stages, while on the surface a concerted hydrogen motion as well as a non-concerted motion is possible. In either case, the barrier height is shown to be much higher than the thermal energy at the experimental temperatures. These results lead to a detailed investigation of the molecular orbitals responsible for the tunneling-induced motion of the central hydrogen atoms. In particular, the evolution of the lowest two unoccupied and nearly degenerate molecular orbitals could be an important piece in the puzzle. Finally, we attempt to develop a simple model that takes into account the electron-induced motion of naphthalocyanine along its switching pathway.

[1] P. Liljeroth *et al.*, Science **317**, 1203 (2007)



## Introduction

-Single-wall carbon nanotube (CNT) is a graphene sheet that has been rolled up to a cylindrical shape. In a unit-cell of graphene there are 2 atoms (A and B) and 2 unit cell vectors  $a_1$  and  $a_2$  as it is shown in the Figure 1.

-Electronic and transport properties of CNTs are sensitive to the side wall adsorbates, particularly to the relative sites that atoms or molecules have been absorbed on. It has been shown in reference 1 that the transport properties do not depend on the type of adsorbate.

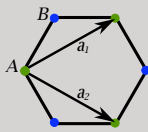


Figure 1. A and B sublattices and the unit vectors ( $a_1$  and  $a_2$ ) of graphene, which can be used for CNTs as well.

-Given two Hydrogen atoms adsorbed on two carbon atoms on the side wall of a metallic CNT, three different cases can be considered:

1. Hydrogen atoms are on two A sites in a way that their relative position ( $R = n a_1 + m a_2$ ) fulfills:

$$n - m = 3p \quad (1)$$

where  $p$  is an integer. In this case the transmission will be reduced from  $2G_0$  to  $1G_0$  around the Fermi energy.

2. Hydrogen atoms have been adsorbed on two A sites but do not fulfill the above condition. Here, the transmission is nearly totally suppressed around the Fermi energy.

3. Hydrogen atoms have been adsorbed on a A and a B site: Unlike two former cases no particular trend has been found for this configuration so far.

-But Hydrogen atoms tend to cluster on the Nanotube surface (Ref. 2). Hence we study the effect of clusters on electronic transport of CNT.

## Results and Discussion

Here we focus on a Hydrogen cluster in which 6 hydrogen atoms are adsorbed on a hexagon of Carbon atoms (Figure 2a). Calculations have been done with both DFT and tight-binding.

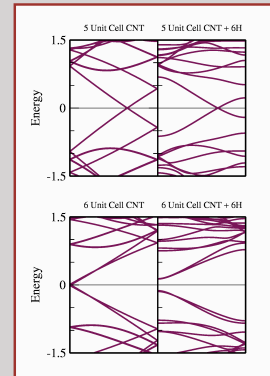
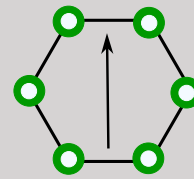


Figure 2. Illustration of (a) the Hydrogen adsorbate cluster, where green circles are Carbon atoms and with circles are Hydrogen atoms, and (b) the bandstructure for 5 and 6 unit cell of CNT(8,8) with and without adsorbates.

-Figure 2b shows the bandstructure of systems of 5 (CNT5) and 6 unit cell CNT (CNT6) both before and after Hydrogen absorption.

-Considering periodic boundary condition, eq.1 has been satisfied (if you take the whole cluster as one object) in CNT6 but not in CNT5. However, unlike single atom adsorbates the band gap has opened in case of CNT6 and not CNT5.

-We observe that the transmission at the Fermi energy has been exponentially reduced with the density of clusters in the central region only if they fulfill the eq.1 (Figure 3).

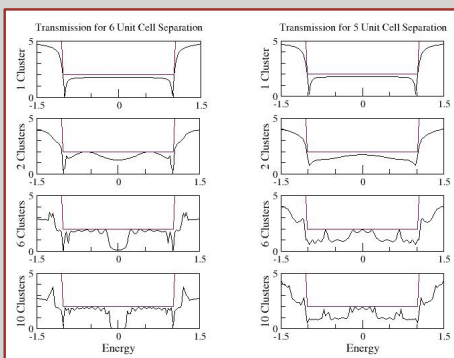
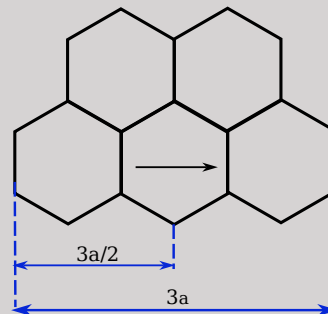


Figure 3. The transmission coefficient for different number of periodic clusters.

-Since the Fermi wavelength of an armchair CNT is  $3a/2$  (with  $a = |a_1|$ ), the exponential decay can be attributed to the destructive interference of the forward moving and reflected electronic wavefunction.



## References

- 1- J. M. García-Lastra, K. S. Thygesen, M. Strange, and Ángel Rubio, Phys. Rev. Lett. 101, 236806 (2008)
- 2- T.T Vehviläinen, M.G. Ganchenkova, V.A. Borodin, R.M. Nieminen, J. Nanosci. Nanotech. 9, 4246-4253 (2009)

# Electronic and magnetic properties of superlattices of graphene/graphane nanoribbons of different edge hydrogenation

A. D. Hernandez-Nieves<sup>(1,2)</sup>, B. Partoens<sup>1</sup>, and F. M. Peeters<sup>1</sup>

<sup>1</sup> Department of Physics, University of Antwerp, Groenenborgerlaan 171, B-2020 Antwerpen, Belgium

<sup>2</sup> Centro Atomico Bariloche, 8400 San Carlos de Bariloche, Rio Negro, Argentina

## Abstract

Zigzag graphene nanoribbons patterned on graphane are numerically investigated by using spin-polarized ab initio calculations.

We found that the electronic and magnetic properties of the graphene/graphane superlattice strongly depends on the degree of hydrogenation on the interfaces between the two materials. When both zigzag interfaces are fully hydrogenated, the superlattice behaves like a zigzag graphene nanoribbon in vacuum, and the magnetic ground state is antiferromagnetic. When one of the interfaces is half-hydrogenated, the magnetic ground state becomes ferromagnetic with possible spintronics applications, whereas the magnetic ground state of the superlattice with both interfaces half-hydrogenated is again antiferromagnetic. In this last case, both edges of the graphane nanoribbon also contribute to the total magnetization of the system. All the spin-polarized ground states are semiconducting, independent of the degree of hydrogenation of the interfaces. Our ab initio results show that the patterned absorption of atomic hydrogen on graphene is a promising way to obtain stable graphene nanoribbons.

## SPIN INELASTIC ELECTRON TRANSPORT THROUGH MAGNETIC NANOSTRUCTURES

A. HURLEY AND S. SANVITO

*School of Physics and CRANN, Trinity College, Dublin 2, Ireland*

A theoretical study has been carried out on the transport properties of single and multiple chains of atomic spins incorporating inelastic interactions. Our calculations are based on the nonequilibrium Green's function formalism with a spin scattering process described within the 1st Born approximation. In particular we calculate the  $I - V$  characteristics and its derivatives both for a single atom of iron [1] as in Fig. 1 and for a one dimensional chain of manganese atoms [2] and we compare with experiment.

We find the same qualitative features as found in experiment, namely the position of the various conductance steps that signify a spin excitation and the parity dependence (even/odd) of the number of atoms in the chain on the conductance profile close to zero bias. More significantly we explain why some excitations are observed and why some are suppressed in the experimental investigation. This is done through a careful derivation of the intensities of given transitions which represent the selection rules for the full spectrum of energy eigenvalues.

## References

- [1] Cyrus F. Hirjibehedin *et al.*, *Large Magnetic Anisotropy of a Single Atomic Spin Embedded in a Surface Molecular Network*, *Science* **317**, 1199 (2007).
- [2] C. F. Hirjibehedin, C. P. Lutz, and A. J. Heinrich, *Spin Coupling in Engineered Atomic Structures*, *Science* **312**, 1021 (2006).

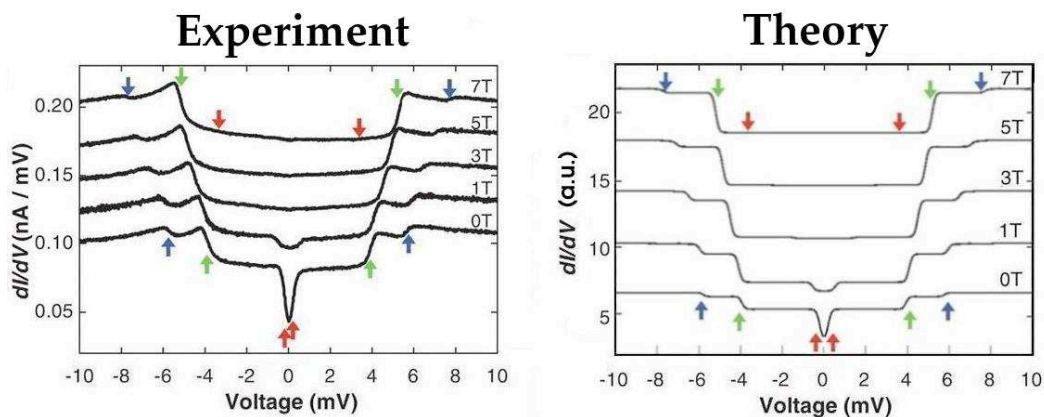


Figure 1: Experimental and theoretical conductance spectra for a single isolated Fe atom under the influence of an external magnetic field applied parallel to the easy axis ( $z$ -axis) of the atom.

# Nanohybrid formed by carbon nanotubes with nucleic acid bases: Raman spectroscopy and *ab initio* calculations

**M.V. Karachevtsev**<sup>1</sup>, S.G. Stepanian<sup>1</sup>, A.Yu. Glamazda<sup>1</sup>

<sup>1</sup>Molecular biophysics department, B.I.Verkin Institute for Low Temperature Physics and Engineering,  
National Academy of Science of Ukraine, Kharkov, 61103, Ukraine

Email: mkarachevtsev@ilt.kharkov.ua

The experimental observation of DNA-carbon nanotube hybrids stimulated a significant interest to these systems due to the possible application of those hybrids as a new generation of bionanosensors. A computer modeling of complexes of DNA and polynucleotides with single walled carbon nanotubes (SWCNT) has been performed in most cases with the use of molecular dynamics methods. These studies revealed the presence of stacking interactions between the nucleic acid bases of DNA with the carbon nanotube surface. An application of more accurate quantum-chemical methods to describe these interactions may provide a more detailed and quantitative characterization of the formation processes and the structures of the DNA-nanotube hybrids.

In this work, we have used Raman spectroscopy and quantum chemical methods (MP2 and DFT) to study the interactions between nucleic acid bases (NABs) and SWCNT. We found that the appearance of the interaction between the nanotubes and the NABs is accompanied by a spectral shift of the high-frequency component of the SWCNT G band in the Raman spectrum to a lower frequency region.

Calculations of the interaction energies between the NABs and a fragment of the zigzag(10,0) carbon nanotube performed at the MP2/6-31++G(d,p)[NABs atoms]/6-31G(d)[nanotube atoms] level of theory while accounting for the basis set superposition error (BSSE) during geometry optimization allowed us to order the NABs according to the increasing interaction energy value. The order is: guanine (-67.1 kJ/mol) > adenine (-59.0 kJ/mol) > cytosine (-50.3 kJ/mol)  $\approx$  thymine (-50.2 kJ/mol) > uracil (-44.2 kJ/mol). The MP2 equilibrium structures and the interaction energies were used as reference points in the evaluation of the ability of various functionals in the DFT method to predict those structures and energies. We showed that the new density functionals (e.g. M05, MPWB1K, MPW1B95) are capable of correctly predicting the SWCNT-NAB geometries but not the interaction energies, while the M05-2X functional is capable of correctly predicting both the geometries and the interaction energies.

Results of this investigation can be applied to development of modern biosensors based on carbon nanotubes.

# Effect of dimensionality on the magnetism of *fcc* Co

P. K. Sahota, P. Manchanda, V. Sharma, A. Kashyap

Condensed Matter Theory Group, The LNM Institute of Information Technology  
Jaipur-302031, (Rajasthan) INDIA



## Motivation

Nanoscale electronic devices are attracting considerable interest due to the impact that they are expected to make in the world of nanotechnology. The most obvious application of nanowires is in electronics and magnetic data storage. Companies are determined to create increasingly tiny transistors, cramming more into smaller chips. There are already computer chips that have nanoscale transistors. Future transistors will have to be even smaller and the result is a nanowire. Nanowires provide an interesting research area because of lot of potential applications such as in electronic and optical devices, magnetic data storage etc. Indeed the origin of magnetism on the nanoscale arises either by reducing the dimensionality of system or by breaking of symmetry. However the magnetization in 3d elements comes only from the spin part because spin orbit coupling does not play much important role in increasing the orbital moment of 3d systems. An example of such type of system is 1D wires of *fcc* Co [1,2].

## Computational Details:

We have applied the fully relativistic linear muffin-tin orbital method within atomic sphere-approximation (LMTO-ASA) to calculate magnetic moments for Co using Barth-Hedin exchange correlation potential [3,4]. Free standing translationally invariant nanowires are built along the [100] direction by periodic repetition of a supercell made up of two *fcc* (100) planes except for monatomic wire. The atomic radii are taken as from bulk value and k-point convergence has been checked. We consider three cases: monatomic wires, 2x2 wire and 5x4 wire as shown in figure below:

## Results:

The calculated spin and orbital magnetic moments of Co nanowires for three cases monatomic, 2x2 wire and 5x4 wire are listed in table 1.

Linear chain	Spin Moment ( $\mu_B$ )	Orbital Moment ( $\mu_B$ )
Bulk Co	1.59	0.23
Monoatomic	2.47	0.82
2x2 wire	1.96	0.12
5x4 wire(I,II, III)	(1.35,1.98,1.73)	(0.03,0.17,0.13)

## Conclusions:

The results show that there is enhancement of magnetic moments as compared to the bulk values, in general, but going from monatomic 1-dimensional wire to 3-dimensional wire, decrease in the magnetic moment is observed.

A substantial redistribution of the charges is seen to occur in 5x4 wire. The atoms which gain charge have lower magnetic moments and atoms which loose charge have higher magnetic moments as compared to bulk value. The atom in the center of the first layer is has more distribution of charge than the corner atoms due to which central one has lower moment

**Acknowledgement:** The research is supported by Department of Science and Technology, New Delhi in form of research project SR/NM/NS-20/2008.

## References:

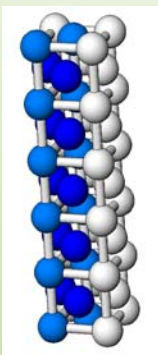
1. T. Sasaki, Y. Egami, T. Ono and K. Hirose, *Nanotechnology* **15** (2004) 1882.
2. J.C. Tung and G.Y. Guo, *Phys. Rev. B* **76** (2007) 094413.
3. O.K. Andersen, *Phys. Rev. B* **12** (1975) 3060.
4. Bao-xing Li and Pei-lin Cao, R. Q. Zhang and S. T. Lee, *Phys. Rev. B* **65** (2002) 125305.

Kashyap

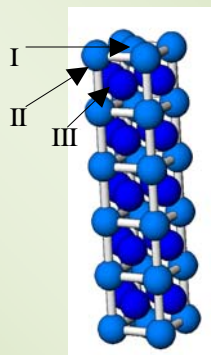
Monatomic wire



Monatomic wire



2x2 wire



5x4 wire

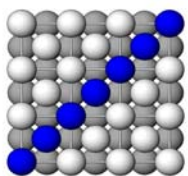
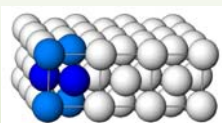
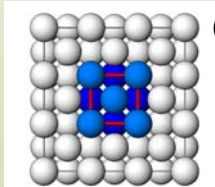


**Figure:** Surface view of different nanowire supercell.

- (a) Top view of monatomic wire. Unit cell in monatomic wire has only one type of metal atom and 64 atoms are taken in unit cell.



- (b) Side view of 2x2 wire. Unit cell in 2x2 wire has only one type of metal atoms and 36 atoms are taken in unit cell.



# Quantum design of new materials: gas molecules under high pressure

Mohammad Khazaei<sup>1</sup>, Mohammad Saeed Bahramy<sup>1</sup>, Fabio Pichierri<sup>2</sup>, Keivan Esfarjani<sup>3</sup>, and Yoshiyuki Kawazoe<sup>1</sup>

<sup>1</sup>*Institute for Materials Research, Tohoku University, Sendai 980-8577, Japan*

<sup>2</sup>*2G-COE Laboratory, Department of Applied Chemistry, Graduate School of Engineering, Tohoku University, Sendai 980-8579, Japan*

<sup>3</sup>*Department of Mechanical engineering, Massachusetts Institute of Technology, Cambridge, MA 02139, USA*

High pressure is a route to explore innovative materials with exotic structures and properties. The recent significant improvements and developments in diamond-cell and shock-tube high-pressure apparatus, and laser heating systems have made it possible to consider the phase transition of materials at high pressure and high temperature in experiments. Simultaneously with above experimental achievements, there has been a substantial theoretical boost in realistic modeling of materials under high pressure and temperature using various quantum mechanical approaches and algorithms. The high-pressure study of phase transitions in solid materials has a relatively long history, but there exists very little knowledge about the behavior of liquids and gaseous molecules under pressure. In this paper, we present our theoretical results on electronic structure of small gas molecules under high pressure. We will discuss how the phase transitions occur at high pressure. The stability of predicted layer and polymer-like structures at ambient pressure is considered by using phonon or MD simulations.

## First-principles study of the Co<sub>2</sub>FeSi(001) surface and Co<sub>2</sub>FeSi/GaAs(001) interface

Sh. Khosravizadeh\*, S. Javad Hashemifar, and Hadi Akbarzadeh  
*Department of Physics, Isfahan University of Technology, 84156-83111 Isfahan, Iran*

*Ab initio* study of the electronic and magnetic properties of bulk Co<sub>2</sub>FeSi, free Co<sub>2</sub>FeSi (001) surfaces, and its interfaces with GaAs (001) substrate are reported. The bulk computations indicate that the LSDA+*U* scheme is necessary to reproduce the measured total magnetic moments and to observe a half-metallic behavior. Hence we applied LSDA+*U* potential and justified *U* parameter to reproduce the correct magnetic moment ( $6\mu_B$ ). Using this *U* parameter, we recalculated the electronic properties of favorable surfaces and interfaces. We used the supercell approach to construct the surface and interface structures. To study surface properties, slabs of 13 layer thickness, 1nm far from each other constructed; surfaces of the slabs used instead of real alloy surface. For interface studies, the interface of 13 layer thick slabs of the alloy with 15 layer thick slabs of the semiconductor used instead. The thermodynamic stability of various Co<sub>2</sub>FeSi (001) surface and Co<sub>2</sub>FeSi/GaAs (001) interface terminations are studied in the framework of *ab initio* thermodynamics. The calculated surface phase diagram indicates that by tuning the atomic chemical potentials, three different terminations are probable. The obtained interface diagrams argue the possibility of the formation of mixed interfaces. The spin-polarized density of states shows that the half metallicity confirmed in the bulk Co<sub>2</sub>FeSi is lost at its surfaces and interfaces with GaAs(001).

# FROM THE REVISION OF BLOCH'S THEOREM TO SPHERICAL DISTORSIONS OF SINGLE- AND MULTI- LAYER GRAPHENE

O. O. Kit and P. Koskinen

Nanoscience Center, P.O.Box 35, FI-40014 University of Jyväskylä, Finland  
[oleg.o.kit@jyu.fi](mailto:oleg.o.kit@jyu.fi)

Boosting the computational research, translational symmetry of Bloch theorem have proven its effectiveness for bulk materials. The more to electronic and mechanical properties' research brings the Bloch's theorem revision, introduced here, valid for any symmetry transformation and particularly useful at nanoscale [1, 2]. Since the low-dimensional structures, instead of translational symmetries, often possess some other symmetries (such as rotational and chiral symmetries for nanotubes and nanotori), Bloch's theorem revision enables proper utilization of these symmetries (e.g. a simulation of a chiral nanotube of any radius from the unit cell of two atoms), leading to considerable economy in computational costs. Moreover, since the effects like bending, twisting and wrapping, being natural attribute of experiment, can be studied from few atoms only (e.g. considering the curvature of bent graphene layer locally), Bloch's theorem revision enables simulation of these structural distortions (e.g. a simulation of twisted nanotube from the unit cell of 2 atoms), providing an easy-access to previously unfeasible systems.

In the poster presentation, we shall present the revision of Bloch theorem and its quick proof, outline the unified formalism for efficient simulations of systems invariant under more general transformation than translation, and the formalism's recent application to spherical bending of single- and multi- layers graphene sheets (Figure 1).

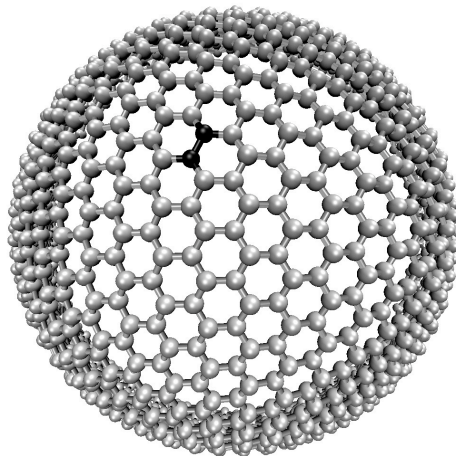


Figure 1. An example illustration of single-layer graphene sheet, bent to the radius of 20 Å. The systems are calculated from the simulation cell of two atoms per layer (depicted in black). The development of easy and efficient simulation formalism naturally follows the work in Ref. 3.

- [1] O. O. Kit *Generalized Symmetries in Nanostructure Simulations*, MSc thesis, Department of Physics, University of Jyväskylä (2009), [available online](#)
- [2] P. Koskinen and O. O. Kit *Simulating distorted nanomaterials: the curvature moduli of graphene* (submitted).
- [3] S. Malola, H. Häkkinen and P. Koskinen *Effects of Bending on Raman-active Vibration Modes in Carbon Nanotubes*, [Phys. Rev. B \*\*78\*\*, 153409 \(2008\)](#)

# First principles molecular dynamics simulations of small peptides on titanium dioxide surfaces

S. Köppen<sup>1,2</sup>, W. Friedrichs<sup>2</sup>, L. Colombi Ciacchi<sup>1</sup>, W. Langel<sup>2</sup>

<sup>1</sup>University of Bremen, Faculty of Production Engineering, Hybrid Materials Interfaces and  
Bremen Center for Computational Material Science

<sup>2</sup>University of Greifswald, Institute of Biochemistry, Biophysical Chemistry

An atomistic picture of the biointerfaces between titanium oxide surfaces and proteins of the extracellular matrix is essential for a detailed understanding of the initial incorporation of titanium-based medical implants within the physiological tissues. In particular, the chemical and physical behaviour of the TiO<sub>x</sub>/collagen interface crucially determines the implant's biocompatibility, while collagen coatings can dramatically enhance the growth of new bone tissue [1]. The adsorption of collagen is mediated by clusters of charged amino acids present in the protein sequence. In collagen fragments, frequently glutamic acid and lysine (GLU-LYS) or aspartic acid and arginine (ASP-ARG) are neighbored [2] and adhere strongly to titanium dioxide surfaces, as found in earlier classical force field simulations [3].

However, due to the fixed distribution of atomic charges in commonly available force fields, it has been so far impossible to investigate the influence of interactions between charged side chains (leading for example to change of point charges of functional group atoms upon formation of intra-molecular hydrogen bonds) on the surface adhesion. Furthermore, the harmonic potentials describing the bonded interactions cannot take into account the dissociation of existing bonds or the building of new ones.

Here we present recent simulations we analyzed the interaction of charged amino acids with titanium dioxide surfaces at the level of Density Functional Theory (DFT). Therefore, we started with simulations of amino acid monomers on titanium dioxide surfaces [4]. In this case it was possible to predict chemical processes like proton transfer

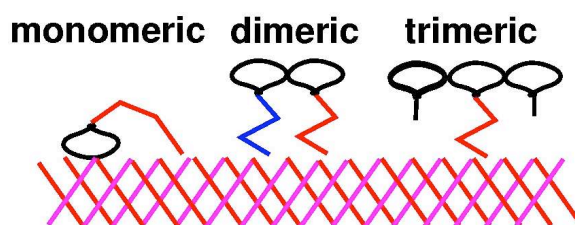


Figure 1

reactions, but the severe size limitation of the monomer models resulted in amino acid adsorption configurations not representative of a peptide. For instance, bridging configurations were obtained, where both the side chain and the backbone interacted with the surface (Fig 1, left). To mimic single contacts of amino acids in a peptide sequence to the surface, at least Tripeptides should be taken into account (Fig 1, right). In a next step we run first principles molecular dynamics simulations of Di- and Tripeptide adhesion reactions on the two most stable rutile surfaces, (110) and (100), and the stable (101) anatase surface. The single contacts of Tripeptides will be compared with the contacts of neighbored charged amino acids contacts (Fig 1, centre) and the charge distribution will be discussed.

- [1] Teng, S., Lee, E., Park, C., Choi, W., Shin, D., Kim, H., *J.Mat.Sci:Mat.Med.* **19** (2008) 2453
- [2] R. Z. Kramer, M. G. Venugopal, J. Bella, P. Mayville, B. Brodsky, H. M. Berman, *J. Mol. Biol.*, **301** (2000) 1191
- [3] S. Köppen, B. Ohler, W. Langel, *Z. Phys. Chem.*, **221** (2007) 3
- [4] S. Köppen, O. Bronkalla, W. Langel, *J.Phys.Chem C* **112** (2008) 13600



# DNA Origami for hybrid nanosensors

Monica Marini, Giuseppe Firrao

Dip.to di Biologia e Protezione delle Piante, Università degli Studi di Udine, via delle Scienze 208, 33100 Udine, Italy



This project is based on the application of DNA based grids to close and open arrays of nanopores on a surface. In this approach, oligonucleotides will interact with a polynucleotide to create ordinate and complex shapes able to change conformation under controlled conditions. The switch mechanism is being initiated by a recognition event where the addition of a target biological molecule works as an activator signal for the opening of the pore. The principles of autonomous base-pairing and the on/off switch of a nanopore, will be applied to create an autonomous molecular machine characterized by its multifunctionality and working in accord to the rules of Boolean Logic.

## Introduction

Hybrid components made of nucleic acids and nano-structured inorganic supports such as nanopores on silicon based membranes, are introducing a new generation of biosensing methods that will avoid the limitations of conventional pathogen detection procedures yet retaining specificity and sensitivity to detect targets without long preliminary steps. In the last years, in our laboratories, strategies have been developed to allow the use of solid state nanopores and the determination of ionic current variation events by analyte-dependent pore clogging. In this context the use of nucleic acid as a constructive material is extremely promising: the new approach here presented is based on the application of switchable, DNA-based origami structure to autonomously close and open nanopores on a silicon based surface.

## Nanopores

The sensing strategy used in the previous work of Moretti *et al.* (2008), is based on the measurement of the ionic current passing through a pore of a silicon based membrane, defining an "ON" or "OFF" state of a switch mediated by molecular interaction. In my project I will use a modified pore using the same working principle: the pore should be surrounded by a gold layer to permit the ligation of the DNA structures to the solid surface mediated by the thiol group of modified oligonucleotides on the edge of the origami structure.

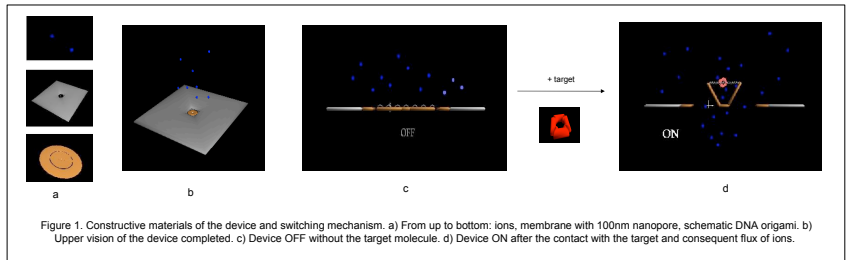


Figure 1. Constructive materials of the device and switching mechanism. a) From top to bottom: ions, membrane with 100nm nanopore, schematic DNA origami. b) Upper vision of the device completed. c) Device OFF without the target molecule. d) Device ON after the contact with the target and consequent flux of ions.

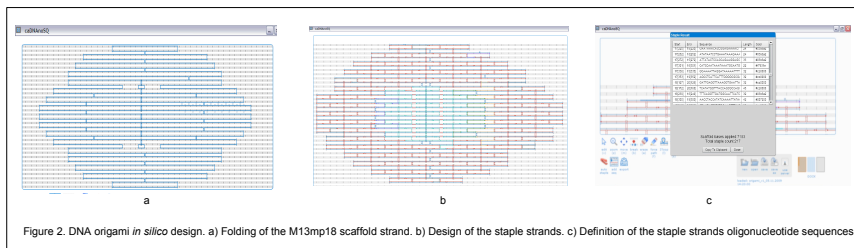


Figure 2. DNA origami *in silico* design. a) Folding of the M13mp18 scaffold strand. b) Design of the staple strands. c) Definition of the staple strands oligonucleotide sequences.

## DNA Origami

Recently, a novel approach to the field of structural DNA nanotechnology was introduced by Rothemund (2006) and named the "DNA origami" method. The 7.2 kb single-stranded DNA viral genome of the M13mp18 bacteriophage (scaffold strand) is folded with the help of 200-250 short synthetic oligonucleotides (staple strands) to create arbitrary two-dimensional rigid and ordinate structures.

In my work the DNA based origami were obtained in three main step. The software package caDNAno (Dietz *et al.*, 2009) was used for the extensive preliminary *in silico* design phase to create the desired origami shape (disks of 100x100nm<sup>2</sup>) and to generate the 218 staple strands nucleotides sequences (Figure 2). In the *in vitro* validation, were optimized the annealing conditions by thermocyclator and the optimal salt concentration in solution. The visualization was made preliminary by agarose gel electrophoresis (Figure 3a) and then with Transmission electron microscopy (TEM, Figure 3b, c, d) and atomic force microscopy (AFM).

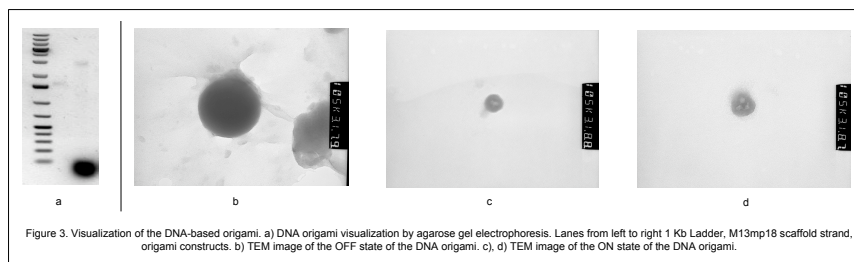


Figure 3. Visualization of the DNA-based origami. a) DNA origami visualization by agarose gel electrophoresis. Lanes from left to right 1 Kb Ladder, M13mp18 scaffold strand, origami constructs. b) TEM image of the OFF state of the DNA origami. c, d) TEM image of the ON state of the DNA origami.

## The switch

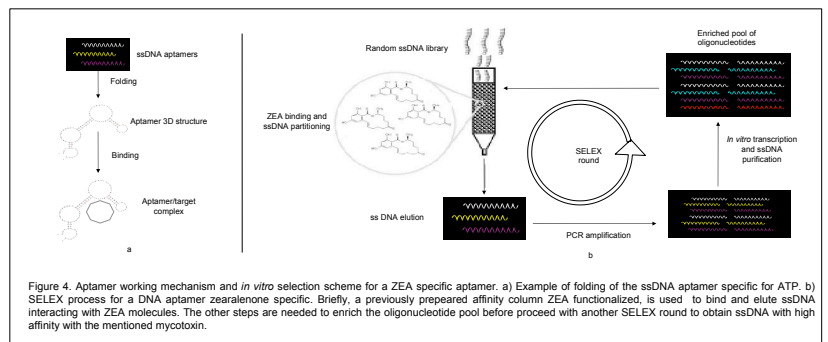
The switch of the structure is based on the change of conformation of a single stranded DNA (ssDNA) linked to the biosensing layer. In this work will be used two approaches; the recognition event can occur through a complementary ssDNA or with a target molecule such as the mycotoxin zearalenone (ZEA). In this last case the ssDNA linked is a specific aptamer. The absence of the biological molecule of interest results in a closed nanopore (OFF); the recognition of the target molecule opens the origami structure and consequently switches ON the nanopore (Figure 1b).

## Aptamers

For a preliminary work will be used a well known aptamer specific for ATP but in the same time an aptamer specific for Zearalenone (ZEA) mycotoxin will be developed in our laboratories. Briefly we adjusted the SELEX protocol for the aptamer selection. Each selection cycle will consist of loading an aliquot of a library of single-stranded DNA oligonucleotides with an internal random sequence onto an affinity column containing ZEA. Modified ZEA will be immobilized on agarose-based resin in presence of DADPA (diaminodipropylamine).

## References

- Dietz, H., Douglas, S.M., Shih, W.M. (2009) Folding DNA into Twisted and Curved Nanoscale Shapes. *Science* 325 (5941): 725-730.
- Moretti, M., Di Fabrizio, E., Cabrini, S., Musetti, R., De Angelis, F., Firrao, G. (2008) An ON/OFF biosensor based on blockade of ionic current passing through a solid-state nanopore. *Biosensors and bioelectronics* 24 (1): 141-147.
- Rothemund, P.W.K. (2006) Folding DNA to create nanoscale shapes and patterns. *Nature* 440: 297 -302.



# Graphene Magnetism probed by $\mu$ SR

M.Mazzani<sup>1</sup>, M.Riccò<sup>1</sup>, D.Pontiroli<sup>1</sup>, J.A.Stride<sup>2</sup>, M.Choucair<sup>2</sup>, O.V.Yazyev<sup>3</sup>

<sup>1</sup> *Università degli Studi di Parma, Dipartimento di Fisica,  
Parco Area Delle Scienze, via G.P.Usberti 7/A, 43100 Parma.*

<sup>2</sup> *University of New South Wales, School of Chemistry, Sydney 2052, Australia.*

<sup>3</sup> *University of California at Berkeley, Department of Physics and Lawrence Berkeley  
National Laboratory, Materials Sciences Division, Berkeley, CA 94720, USA.*

Graphene, the 2-dimensional allotrope of carbon, displays unique electronic and transport properties, which are attracting a great interest from the perspective of both fundamental physics and technological applications. Nevertheless a description of its magnetic properties still lacks and, more generally, the possibility of magnetic interactions in pure carbon materials is a strongly debated issue within the scientific community.

We have investigated macroscopic quantities of graphene, prepared by different chemical methods, by  $\mu$ SR (Muon Spin Rotation/Relaxation). The observation of muon spin precession in all of these samples gives a clear indication of the presence of *long range magnetic order in graphene*. The muons probe a relatively small hyperfine local field, in the range of 4-8 G and the magnetic order proves to be thermally stable: at 600 K only 40% reduction of local magnetization is observed. The magnetic volume fraction is sample dependent and acquires up to 15% of the sample. SQUID magnetometry and the measured dependence of local field on an externally applied magnetic field, suggest that the magnetic order is of antiferromagnetic type.

A clear correlation between the magnetic signal amplitude and the defect concentration, estimated by Raman and SQUID magnetometry, suggests that the in-plane defects could be the origin of the magnetic phase. *First-principle calculations* have been performed to relate these defects and the observed hyperfine interactions.

# Wettability at nanoscale: a molecular simulation study

Caetano R. Miranda

Universidade Federal do ABC - Centro de Ciências Naturais e Humanas  
Rua Santa Adélia, 166 - Bairro Bangu - Santo André - SP – Brazil – 09210-170  
e-mail: caetano.miranda@ufabc.edu.br

The current understanding of wettability phenomena at nanoscale is still on debate [1]. Most of the available results on interfacial energy do not include the size effect and surface morphology, which come out to be crucial at nanoscale. In this work, we have performed a study of the water/oil/nanoparticles three-phase interfaces using a combination of First Principles calculations with Classical Molecular Dynamics. Using first principles based optimized interatomic potentials [2,3], we have systematically calculated the contact angle of oil nanodroplets (2-5 nm diameter) on top of SiO<sub>2</sub> amorphous surface under solvent (H<sub>2</sub>O). The interfacial energy between SiO<sub>2</sub> nanoparticles under H<sub>2</sub>O with different NaCl concentration was also determined using a combination of non-equilibrium free energy methods (Adiabatic Switching and Reversible Scaling). Combined with our experimental data [4], the simulation results not only help to understand the fundamentals of wettability at nanoscale, but also is crucial for applications on optimizing oil recovery.

[1] J. F. Kuna, et al., *Nature Materials*, 8, 837 (2009)

[2] P. Tangney and S. Scandolo, *J. Chem. Phys.* 117, 8898 (2002).

[3] M. F. Michelon, and C. R. Miranda, in preparation.

[4] D. Makimura, C. Metin, T. Kabashima, T. Matsuoka, Q. Nguyen, C. R. Miranda, submitted to *Journal of Materials Science* (2009).

**Title: Thermo-Mechanical properties of defected graphene**

---

**M. NEEK-AMAL**

Abstract:

Mechanical stiffness of defected monolayer graphene is studied using molecular dynamics simulation and theory of elasticity. The nanoindentation is used for calculating Young's modulus. Randomly distributed vacancies in the surface of circular monolayer graphene with clamped boundary condition reduce the mechanical stiffness of the sheet. Young's modulus of graphene decreases linearly versus the percentage of vacancies in a surface having 15 nm of radius. Also the effective spring constant of circular monolayer graphene decreases by increasing the percentage of vacancies. The load and unload curves are the same as usual perfect monolayer graphene. The breaking force decreases in the defected cases and breaking points depend on the percentage of vacancies and fracture may be appeared near the boundaries. We introduce a simple method for vibrating the system by pulling slowly up the AFM tip over the center of clamped circular monolayer graphene and obtained frequencies of vibration.

## Introduction

- Perovskites have a simple structure (Fig. 1) and exhibit interesting polarization, dielectric and electromechanic properties: they are very **sensitive to small deformations**.

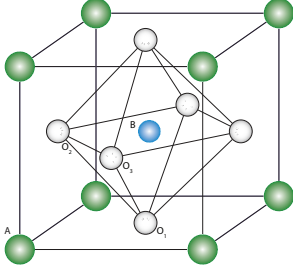


Figure 1: General perovskite ( $\text{ABO}_3$ ) in the high symmetry cubic (non-polarized) phase.

- Perovskites are used in solid state memories, sensors, capacitors and other electronic components.
- $\text{NaNbO}_3$  and  $\text{SrTiO}_3$  are perovskites very close to the ferroelectric phase transition, and exhibit complex structures with rotations of the oxygen octahedra.

## Superlattice properties

- Perovskite superlattices have stacked, epitaxial layers of different perovskites. They may have properties that cannot be achieved in single perovskites, e.g. increased polarization and permittivity.
- $\text{NaNbO}_3$  and  $\text{SrTiO}_3$  thin films have very similar bulk lattice constants, 3.908 Å and 3.905 Å, respectively. Therefore,  $\text{NaNbO}_3/\text{SrTiO}_3$  superlattices have **no misfit strain**, and the behavior of the structure is determined solely by subtler **interface effects**.
- The  $\text{NaNbO}_3/\text{SrTiO}_3$  (100) interface is **charge-imbalanced**:  $\text{SrO}$  and  $\text{TiO}_2$  layers are charge neutral, while  $(\text{NaO})^-$  and  $(\text{NbO}_2)^+$  layers are charged if we consider their preferred ionic charges (Fig. 2). Therefore,  $\text{SrO-NbO}_2$  interface (denoted  $n$ ) has half an extra electron, while  $\text{NaO-TiO}_2$  interface (denoted  $p$ ) has half a hole compared to nominal ionic charges.

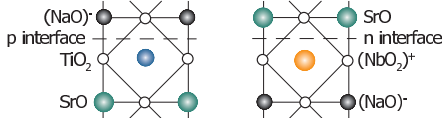


Figure 2: The two possible interfaces between  $\text{SrTiO}_3$  and  $\text{NaNbO}_3$ .

- Charge-imbalanced interfaces are known to have **rich behavior**: a high-mobility 2D electron gas has been observed in the  $\text{LaAlO}_3/\text{SrTiO}_3$  interface [1], leading to metallicity in-plane. Lattice relaxation from the ideal perovskite positions has been calculated to be considerable in such interfaces [2].
- $\text{NaNbO}_3/\text{SrTiO}_3$  superlattices are reported to have **anomalous properties** such as expansion of volume and decrease of permittivity [3].

## Calculated systems

- We consider [4] eight simple  $\text{NaNbO}_3/\text{SrTiO}_3$  superlattice structures (Fig. 3).
- We account for lattice relaxation and the effect of octahedral rotations and other low-symmetry structures.

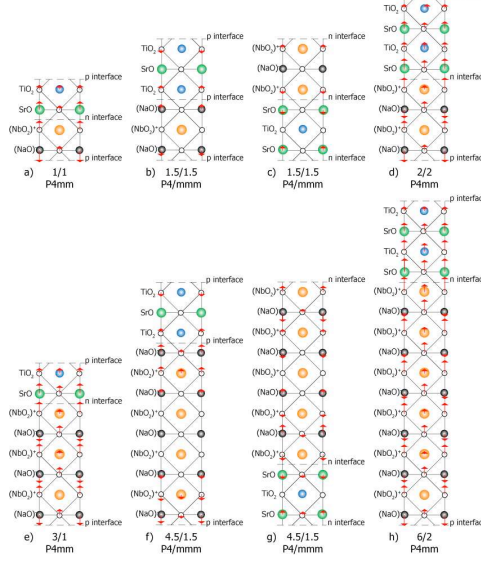


Figure 3: The eight superlattices considered. Red arrows indicate direction and magnitude of displacement, when the ionic positions are relaxed within the high-symmetry space group. For each structure, the number of  $\text{NaNbO}_3/\text{SrTiO}_3$  layers is given, along with the high-symmetry space group. a.d.e.h) Those with integer number of layers have two different interfaces and are free to relax in the  $z$  direction. b.e.f.g) Those with non-integer number of layers have two similar interfaces, which will result in one extra electron or hole in the superlattice. Their mirror symmetry restricts relaxation in  $z$ .

## Method

- VASP, PAW, LDA/LSDA+U, 700 eV cutoff
- $\Gamma$  and  $M$  point phonons using the frozen phonon method. Unstable phonons coupled to find zero-T ground state.

## Results

- Relaxation of positions (red arrows in Fig. 3) opens up a **band gap**.  $n$  interface cubic cell will expand,  $p$  interface cell contract.  $\text{SrTiO}_3$  cell will contract.
- Nb centered octahedra will rotate around all cubic axes, Ti centered around  $x$  and  $y$ . This is likely to be the preferred phase at room  $T$ .

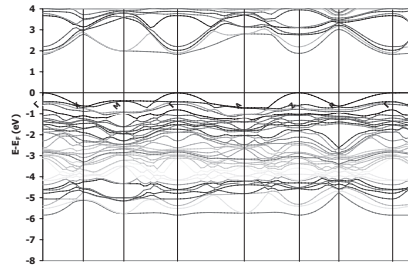


Figure 4: LDA band structure of the relaxed 1/1  $\text{NaNbO}_3/\text{SrTiO}_3$  superlattice in the monoclinic  $P_a$  phase (rotated octahedra). Fermi level is set at HOMO. The pseudotetragonal Brillouin Zone points are  $\Gamma=(0,0,0)$ ,  $X=(1/2,0,0)$ ,  $M=(1/2,1/2,0)$ ,  $A=(1/2,1/2,1/2)$ ,  $R=(1/2,0,1/2)$  and  $Z=(0,0,1/2)$ .

- In superlattices with **two different interfaces** (a,d,e,h in Fig. 3) there are no extra electrons or holes compared to nominal charges, and the structures are **insulators**. Buckling of layers is large. Example band structure is shown in Fig. 4.
- In superlattices with **two n interfaces/two p interfaces** (b,c,f,g in Fig. 3), there is one electron above/one hole below the gap, making the structure **metallic**.
- The conduction hole is in oxygen  $p_x p_y$ ,  $p_x p_z$  or  $p_y p_z$  orbitals, mostly in  $\text{SrTiO}_3$  layer, while the conduction electron occupies both Nb and Ti  $d_{xy} d_{xz} d_{yz}$  orbitals, as displayed in Fig. 5.
- LSDA+U yields **half-metallicity** and ferromagnetic alignment for holes, but not electrons.
- Superlattices which have **two n interfaces/two p interfaces** have all lattice parameters increased/decreased. This is because they contain a larger percentage of large/small ions.

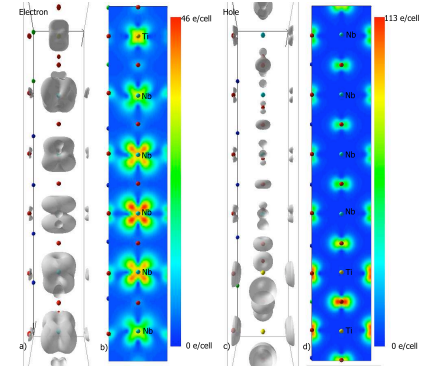


Figure 5: Charge density isosurfaces (at 5 e/cell) and charge density plots (in logarithmic scale) for the single electron above the gap in 4.5/1.5  $n$  superlattice (a and b) and the single hole below the gap in 4.5/1.5  $p$  superlattice (c and d). The structures are in high symmetry  $P4/mmm$  phase.

## Conclusions

- As simple band theory would suggest, superlattices with two similar interfaces are metallic.
- Conduction holes are more localized in  $z$  than conduction electrons, so 2D/3D metallicity may be influenced by interface type and layer thicknesses [4].
- Buckling, volume expansion, and polar distortions occur near interface. This may lead to an interface layer with permittivity different from bulk [5].

## Acknowledgements

This work was funded by the Academy of Finland and the Finnish Academy of Science and Letters.

## References

- A. Ohtomo and H. Y. Hwang. A high-mobility electron gas at the  $\text{LaAlO}_3/\text{SrTiO}_3$  heterointerface. *Nature*, 427:423, 2004.
- S. Okamoto, A. J. Millis, and N. A. Spaldin. Lattice relaxation in oxide heterostructures:  $\text{LaTiO}_3/\text{SrTiO}_3$  superlattices. *Phys. Rev. Lett.*, 97:056802, 2006.
- J. Narkilahti, M. Plekh, J. Levoska, and M. Tyunina. Anomalous growth and properties of  $\text{SrTiO}_3\text{-NaNbO}_3$  superlattices. *Phys. Rev. B*, 79:014106, 2009.
- R. Oja and R. M. Nieminen. Modeling charge-imbalanced  $\text{NaNbO}_3/\text{SrTiO}_3$  superlattices: Lattice relaxation and metallicity. *Phys. Rev. B*, 80:205420, 2009.
- M. Tyunina, M. Plekh, R. Oja, and R. M. Nieminen. Submitted to *Appl. Phys. Lett.*

## **A Numerical Model for Determination of Electrostatic Charge Distribution on Conducting Nanowires**

**Masoume OZMAEIAN**

**Abstract:** In this paper charge distribution in conducting nanowires and nanotubes has been studied theoretically. The proposed model is based on classical electrostatics. This numerical model overcomes the problem of dealing with different kinds of applied electric fields and nanowire geometries. Charge distribution is obtained by dividing the nanowire into smaller elements with a centre of effective electric charge. In this paper, different kinds of geometrical elements are investigated which are useful for straight and bent nanowires with different aspect ratios. Numerical results are presented for selected examples which are in good agreement with those of obtained by density functional theory in previous studies. The findings are useful for analysis of electromechanical systems.

**Keywords:** charge distribution; nanowire; electric field.

# *Ab initio* calculations for the electrostatic field effects on the electronic properties in some phenylene based oligomers

Irina Petreska<sup>1</sup>, Ljupčo Pejov<sup>2</sup> and Ljupčo Kocarev<sup>3</sup>

<sup>1</sup>*Institute of Physics, Faculty of Natural Sciences and Mathematics,  
Ss. Cyril and Methodius University,  
PO Box 162, 1000 Skopje, Republic of Macedonia,  
e-mail:irina.petreska@pmf.ukim.mk*

<sup>2</sup>*Institute of Chemistry,  
Faculty of Natural Sciences and Mathematics,  
Ss. Cyril and Methodius University,  
Arhimedova 5, PO Box 162,  
1000 Skopje, Republic of Macedonia*

<sup>3</sup>*Macedonian Academy of Sciences and Arts,  
bul.Krste Misirkov 2. PO Box 428 1000 Skopje,  
Republic of Macedonia*

(Dated: December 30, 2009)

**Abstract.** First principles molecular orbital theory was used to investigate the electric field effects on the electronic properties of some bistable phenylene based oligomers. Two kinds of phenylene oligomers were considered, first the basic phenylene ethynylene oligomer (OPE), without permanent dipole momentum, and then a sample containing dipolar side group. We were concentrated on the field effects on the properties related to molecular electronic conductance, such as potential barrier height, HOMO-LUMO gap, and intramolecular torsional dynamics. For that purpose electrostatic fields having various magnitudes and orientations were explicitly included in the Hamiltonian of the considered system, and the Schrödinger equation was iteratively solved. In both oligomers, interesting effects of the applied fields on the potential energy surface, HOMO-LUMO gap, and transition probabilities were observed, and the possibility to modulate and control the single-molecule switching was evident. In the basic OPE external field directed perpendicularly to the molecular plane was shown to induce conductance switching, while an electric field directed along axis lying within the molecular plane and being perpendicular to the principal molecular axis was shown to be capable of controlling the stochastic conductance by a strong modulation of the corresponding classical transition probability. Similar effects were observed in the oligomer containing dipolar side group. The major difference between the two kinds of oligomers is that in the one containing dipolar side group, the probability for quantum tunneling is more pronounced than the classical transition probability. Having on mind that the second oligomer has permanent dipole momentum, the field effects in this case will be dependent not only on the field orientation, but also on its direction.

*Keywords:* phenylene ethynylene oligomers, molecular conductance, HOMO-LUMO gap, intramolecular torsions, frontier molecular orbitals, density functional theory.

# **First-Principles Study of Structural Stability and Electronic Structure of CdS Nanoclusters**

**S. Datta (1,2), M. Kabir (1,3), D. D. Sarma (4) and T. Saha-Dasgupta(1)**

*1. S.N. Bose National Centre for Basic Sciences, Kolkata 700098, India*

*2. CAMD, Dept. of Physics, Building 307, DTU, DK-2800 Kongens Lyngby, Denmark*

*3. Department of Materials Science and Engineering, Massachusetts Institute of Technology, USA*

*4. Solid State and Structural Chemistry Unit, Indian Institute of Science, Bangalore 560012, India*

Using first-principles density functional calculations, we have studied the structural stability of stoichiometric as well as nonstoichiometric CdS nanoclusters at ambient pressure with diameters ranging up to about 2.5 nm. Our study reveals that the relative stability of the two available structures for CdS, namely zincblende and wurtzite, depends sensitively on the details like surface geometry and/or surface chemistry. The associated band gap also exhibits nonmonotonic behavior as a function of cluster size. Our findings may shed light on reports of experimentally observed structures and associated electronic structures of CdS nanoclusters found in the literature.

# TRANSPORT PROPERTIES OF PROTRUDED GRAPHENE NANORIBBONS

K. Salorittu,<sup>1</sup> Y. Hancock,<sup>1,2</sup> A. Kärkkäinen,<sup>3</sup> L. Kärkkäinen,<sup>3</sup> A.-P. Jauho,<sup>1,4</sup> and M.J. Puska<sup>1</sup>

## Graphene nanoribbons

**Graphene** Recent advances [1] have permitted the experimental study of single-layer graphene on a SiO<sub>2</sub> substrate, leading to an exploding theoretical interest in this novel two-dimensional material. The current interest in graphene is mostly due to

- A linear energy dispersion near the Fermi level, hence
  - A relativistic Dirac Hamiltonian
  - An anomalous quantum Hall effect
  - The possibility to test relativistic effects like the Klein paradox
- A high quality lattice due to strong carbon-carbon bonding with
  - Long mean free path
  - Long coherence length
  - High mobility up to room temperatures
  - Electronic applications: graphene FETs, electron waveguides etc.

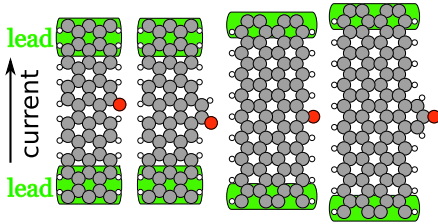
**Nanoribbons** A sheet of graphene is a zero-gap semiconductor and thus unsuitable for many logic applications. A band-gap can be generated, however, by cleaving the sheet to finite strips, i.e., graphene nanoribbons (GNRs). Nanoribbons have been realized experimentally [2] and recently sub-10 nm ribbons with smooth edges have been created via chemical means [3].

GNRs can be divided to two ideal classes, armchair (AGNR) and zigzag (ZGNR), based on the type of the edge. The nature of the edge has a large impact on the electronic and transport properties of GNRs and thus the effect of different adsorbents and dopants has recently come under intense study [4].

## Our study

### Systems

- Ideal armchair and zigzag graphene nanoribbons with adsorbed oxygen.
- Non-ideal armchair and zigzag GNRs with protrusions (GNR-prot) and adsorbed oxygen.



### Methods

- Density-functional theory (DFT) ground-state calculations for a supercell geometry with SIESTA [5]
  - GGA-PBE xc-functional
  - DZP orbitals, 400 Ry mesh cutoff
  - 30 k-points
  - Structures relaxed to 0.01 eV/Å
- Nonequilibrium Green's functions and DFT zero-bias transport calculations for a two-probe geometry with TranSIESTA [6]
  - SZP orbitals, 125 Ry cutoff

## Adsorption

system	O ads. energy (eV)
AGNR	5.93
ZGNR	7.46
ZGNR-prot	6.04
AGNR-prot	6.48

- Zigzag edge is highly reactive due to edge states.
- Protrusion suppresses the edge states, leading to a much diminished adsorption.

- In comparison, for the armchair edge, the protrusion causes a considerable increase in the adsorption.

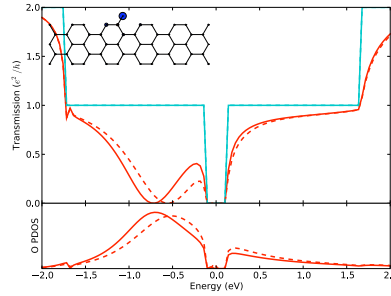
## Transport

We calculate the transmission function

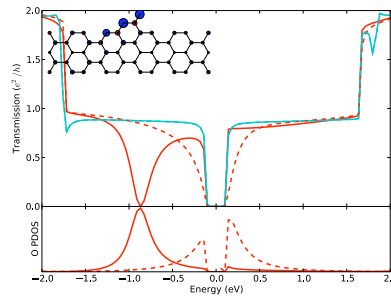
$$T(\omega) = \text{Tr}\{\Gamma_L G^R \Gamma_R G^A\},$$

where  $\Gamma_{L/R}$  are the lead coupling terms and  $G^{r/a}$  are the retarded/advanced Green's functions.

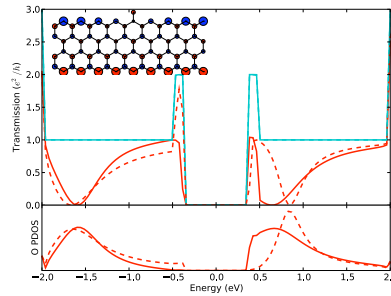
- Red: system with adsorbed oxygen
- Magenta: system with oxygen replaced by hydrogen
- Dashes: the second spin channel transmission when this differs from the first
- Insets show the structures and spin-up minus spin-down Mulliken charges, i.e. charge projected on the atomic orbitals.



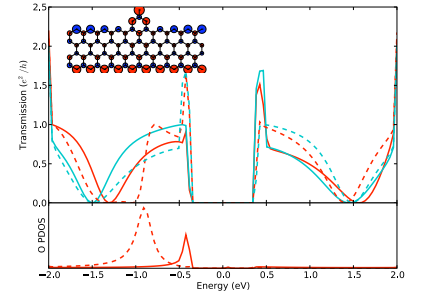
The dip in the transmission corresponds perfectly with a peak in the oxygen partial density of states (PDOS), indicating Fano antiresonance, i.e. localized states of the oxygen orbitals are interfering with the continuum Bloch states of the nanoribbon [7]. The breaking of the spin degeneracy is due to the way oxygen orbitals are filled, which leads to a spin polarized Mulliken charge difference as seen in the inset.



The strongly peaked oxygen spin-up PDOS suppresses one spin channel entirely while leaving the other unaffected. The spin polarized Mulliken charge is more delocalized.



In contrast with the AGNR results the bonding with the oxygen suppresses the spin polarized edge-states and the oxygen PDOS is also not very spin polarized. The Fano antiresonance explanation for the dips in the transmission curve remains valid.



For the protruded zigzag ribbon the transmission is no longer dominated by the Fano antiresonance with oxygen states but the protrusion itself dominates transport.

## Summary

### Conclusions

- Protrusions in AGNRs have the highest adsorption energy for atomic oxygen, followed by plain ZGNRs, ZGNR protrusions and finally plain AGNRs.
- The transport properties are heavily affected by the addition of adsorbates, particularly via the introduction of Fano antiresonances on the transmission function.
- For the armchair ribbons introduction of edge disorder is relatively unimportant and the chemical disorder of the oxygen adsorbent dominates the transmission characteristics.
- For the zigzag ribbon edge disorder is the most important factor and the adsorbent is of lesser impact.

### Affiliations

- <sup>1</sup>Department of Applied Physics, Helsinki University of Technology  
<sup>2</sup>Department of Physics, University of York  
<sup>3</sup>Nanosystems, Nokia Research Center  
<sup>4</sup>Department of Micro and Nanotechnology, Technical University of Denmark

### References

- [1] K. S. Novoselov *et al.*, *Science* **306**, 666 (2004).
- [2] M. Y. Han, B. Ozyilmaz, Y. Zhang, and P. Kim, *Physical Review Letters* **98**, 206805 (2007).
- [3] X. Li, X. Wang, L. Zhang, S. Lee, and H. Dai, *Science* **319**, 1229 (2008).
- [4] F. Cervantes-Sodi, G. Csányi, S. Piscanec, and A. C. Ferrari, *Physical Review B* **77**, 165427 (2008).
- [5] J. M. Soler *et al.*, *J. Phys.: Cond. Matt.* **14**, 2745 (2002).
- [6] M. Brandbyge, J.-L. Mozos, P. Ordejón, J. Taylor, and K. Stokbro, *Physical Review B* **65**, 165401 (2002).
- [7] U. Fano, *Phys. Rev.* **124**, 1866 (1961).

## **A Classical Potential to Model Protein Adsorption on Natively Oxidised Titanium Surfaces**

Julian Schneider and Lucio Colombi Ciacchi,

*Hybrid Materials Interfaces Group, University of Bremen, Bremen, Germany*

In order to investigate the surface properties of metals in a realistic fashion it is crucial to take into account the thin oxide layer that forms spontaneously when the surface is exposed to an oxidising environment. Starting from reference oxide layer structures obtained in extensive first-principles molecular dynamics simulations, we have developed a novel classical potential which is able to reproduce the topological binding features of the amorphous oxide network on Ti as well as the interfacial behaviour of the TiO<sub>x</sub>/water interface. The analytic form of the potential has been chosen so that it can be easily combined with well-established biomolecular force fields. This allowed us to perform classical simulations of small organic molecules on the oxide surface and compare the results with those of density functional theory calculations. Ongoing work is focusing on the application of our force field to simulate the adsorption of amino acids, small peptides and larger protein fragments on oxidised Ti surfaces.

# Innovative Latent Heat Thermal Storage Elements Design Based On Nanotechnologies

Giacomo Sciuto, Roberto Muscia

Mechanical Engineering Department, University of Trieste, Trieste, Italy

Spring College on COMPUTATIONAL NANOSCIENCE 17-28 MAY 2010 - ICTP TRIESTE



UNIVERSITA' DEGLI STUDI DI TRIESTE  
GRADUATE SCHOOL OF NANOTECHNOLOGY  
ELCON ELETTRONICA s.r.l.

## Objectives

The main objective of this research activity is the development of a thermal storage system that may accumulate energy surplus coming from solar thermal panels during daytime and that may return the collected energy in nighttime or during peak demand.

PCMs (Phase Change Materials) could be considered very good candidates for this usage. PCMs possess a great capacity of energy accumulation around melting temperature thanks to the latent heat. In spite of this great potential, the practical feasibility of latent heat storage with PCM is still limited, mainly due to a rather low thermal conductivity. This (low conductivity) implies small heat transfer coefficients and, consequently, thermal cycles are slow and not suitable for most of the potential applications.

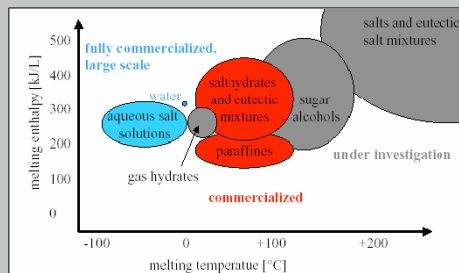


Figure: Available PCMs

## Methods

There are basically two strategies to improve heat exchange:

- ▶ optimizing heat exchange surfaces (e.g. using fins);
- ▶ doping PCM with highly conductive additives (e.g. inserting graphite powder).

## Effect of macro-doping on heat exchange

An optimized modular heat exchanger, for hot water production, has been (numerically) tested using on one hand a commercially available pure PCM (Rubitherm Paraffin Wax RT65) and on the other hand the same PCM doped with macro-additives (Rubitherm Paraffin Wax RT65+CENG -Compressed Expanded Natural Graphite).

Table: PCM and PCM-CENG physical properties

	RT65	RT65+CENG
Density	700[kg/m <sup>3</sup> ]	600[kg/m <sup>3</sup> ]
Melting Temperature	338 ± 2[K]	338 ± 2[K]
Latent Heat	170000[J/kg]	150000[J/kg]
Thermal Conductivity	0.2[W/mK]	15[W/mK]
Specific heat capacity	1800[J/kgK]	1800[J/kgK]

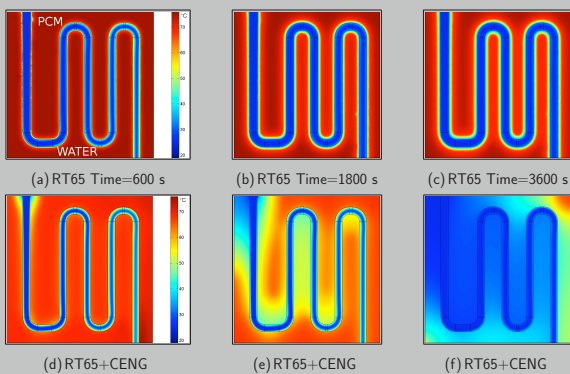


Figure: Temperature field inside heat exchanger

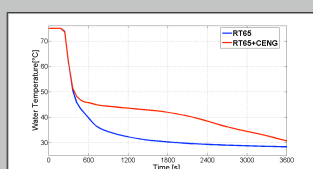


Figure: Temperature of out flowing water

- ▶ The heat transfer from PCM to water is very poor without CENG and water receives only a very low part of thermal energy;
- ▶ Despite the lower latent heat, the CENG-PCM system is more efficient.

## Nano-doping

The possibility of exploiting highly conductive nano-additives as doping material has been investigated.

Thanks to their small size, nano-particles, can be dispersed inside the PCM better than macro or micro elements.

## Materials, sample preparation and experimental setup

- ▶ Single Walled Carbon Nanotubes (by Helix Material Solution) with high purity (90%), diameter  $\phi = 1.3 \text{ nm}$  and length  $L = 0.5 - 40 \mu\text{m}$ ;
- ▶ Commercial Paraffin Wax, with melting temperature of 57°C;
- ▶ Several mixtures (pure PW, 0.1% - 0.2%... till 2% CNTs);
- ▶ 4 hours sonication at 75°C;
- ▶ 24 hours cooling time at room temperature;
- ▶ DSC analysis (Q100) between 42°C and 70°C;
- ▶ Ramp signal 2°C/min;

## Results

Table: DSC collected data

PCM	CNT mass Frac.	Measured Latent Heat	Enhancement	Theoretical Latent Heat
Pure PW	0	122.10 [J/kg]	-	122.10 [J/kg]
CNT 0.1	0.1%	123.13 [J/kg]	0.84%	121.98 [J/kg]
CNT 0.5	0.5%	125.60 [J/kg]	2.87%	121.48 [J/kg]
CNT 0.8	0.8%	127.55 [J/kg]	4.46%	121.12 [J/kg]
CNT 1	1%	129.05 [J/kg]	5.69%	120.87 [J/kg]
CNT 2	2%	131.00 [J/kg]	7.29%	119.66 [J/kg]

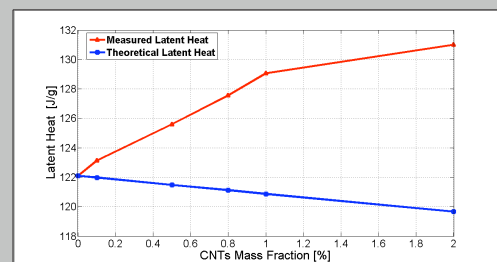


Figure: DSC profiles of nano-doped PCMs

## Conclusion

- ▶ Nano-doping demonstrates an enhancement of latent energy storage of PCMs, unlike what happens with macro-doping; this improvement can be caused by intermolecular attraction between the molecules of nano-additives and wax;
- ▶ A similar enhancement is expected on the thermal conductivity;
- ▶ Highly conductive nano-particles seem to be very good candidates for doping thermal storage materials.

## Acknowledgements

Thanks to Chiara Fabbro and Maurizio Prato for their collaboration during DSC analysis.

Thanks to Veronica Simeone for the linguistic revision.

Thanks to ELCON Elettronica s.r.l. that funded this research.

## References

- H. MEHLING, S. HIEBLER, F. ZIEGLER, *Latent heat storage using a PCM-graphite composite material*.
- D. HAILLOT, X. PY, V. GOETZ, M. BENABDELKARIM, *Storage composites for the optimisation of solar water heating systems - Chemical Engineering Research and Design* 86, (2008) 612-617.
- H. MEHLING, L. F. CABEZA, *Heat and cold storage with PCM. An Up to date introduction into basics and applications - Ed. Springer*, (2008).
- S. SHAIKH, K. LAFDI, K. HALLINAN, *Carbon nanoadditives to enhance latent energy storage of phase change materials - Journal of Applied Physics* 103, (2008).
- J. WANG, H. XIE, Z. XIN, *Thermal properties of heat storage composites containing multiwalled carbon nanotubes - Journal of Applied Physics* 104, (2008).
- J. WANG, H. XIE, Z. XIN, *Thermal properties of paraffin based composites containing multi-walled carbon nanotubes - Termodinamica Acta* 488, (2009).

## **Interfacial roughness in resonant tunneling of double-magnetic barriers quantum wells**

**Aliasghar Shokri**<sup>1</sup>

Department of Physics, Payame Noor University (PNU), Nejatollahi Street, 159995-7613 Tehran, Iran

Computational Physical Sciences Research, Laboratory, Department of Nano-Science, Institute for Research in Fundamental Science (IPM),

P. O. Box 19395-5531, Tehran, Iran

**ZH. Ebrahiminejad**

Department of Physics, K.N. Toosi University, 41, Shahid Kavian St., 15418-49611 Tehran, Iran

The Influence of interfacial roughness on spin-dependent resonant tunneling through a nonmagnetic (NM)/EuS double-magnetic barrier structure (NM/EuS/NM/EuS/NM) are investigated in the coherent regime. In our calculation, we treat the rough potential as a periodic surface corrugation models. Based on the transfer matrix method, the transmission probabilities are calculated for the perfect and non-perfect (direct and indirect components) interfaces within the framework of the effective mass approximation. The results show an oscillatory behavior for TMR and spin polarization (SP) as a function of the width of quantum well due to the resonant states in the NM layer. Because of electron scattering in the non-perfect case, these oscillations are more obvious. According to our results, the TMR and SP reach to about 99% and 100%, respectively at zero temperature in the perfect case. With increasing the thickness of NM layer, the position of resonant energies for the current components becomes different in all configurations, so the regular behavior of TMR and spin polarization changes. Because of the conductivity of the parallel configuration is larger than antiparallel, the absolute value of TMR increases in some situations. Also, the interface roughness/islands degrade the transmission probability. This model could be generalized for present interface roughness in multi-wells structures in designing the spintronics devices.

**keywords:** Interfacial roughness; Spin polarized transport; Resonant tunneling; double-Magnetic barrier

---

<sup>1</sup> Corresponding author, E-mail: [aashokri@tehran.pnu.ac.ir](mailto:aashokri@tehran.pnu.ac.ir)

# Chitosan on Co Nanoparticles: an *Ab Initio* Study

P.L. Tereshchuk<sup>1,2,3</sup>, M. Thorwart<sup>1</sup>, N.N. Turaeva<sup>2</sup>, S.Sh. Rashidova<sup>2</sup>

<sup>1</sup>Freiburg Institute for Advanced Studies (FRIAS), Albert-Ludwigs-Universität Freiburg, Freiburg, Germany

<sup>2</sup>Institute of Chemistry and Physics of Polymers, Tashkent, Uzbekistan

<sup>3</sup>Institute of Nuclear Physics of Uzbekistan, t. Ulugbek, Tashkent, Uzbekistan

**Introduction.** Transition metal *nanoparticles* (NP) are an attractive subject of research because of their unique electronic and magnetic properties that substantially differ from a bulk material. An unusual enhanced magnetic moments of the NP from their bulk values result from surface and quantum sized effects. In addition NP stabilized by *organic molecules* are of a great interest for basic science and some applications due to the possibility combining chemical and physical properties of both organic molecule and metal NP. However, a contribution of the organic material to magnetic properties of NP in consequence of atomic interactions of molecule and NP can lead to essential changing properties for such NP.

**The aim of research.** Co-NP joined with a chitosan molecule have been investigated to understand the influence of the molecule on stabilization and magnetic properties Co-NP.

**Method.** Properties of Co+chitosan NP have been studied using density functional theory (OPENMX code [1]). In our calculations a chitosan molecule represents dimer- and trimer-chitosan polymers. A basis of pseudoatomic orbitals including minimal basis of *s*-functions of hydrogen atoms, *p*-orbitals of carbon atoms, *s*2*p*2*d*2 and *s*2*p*2*d*2*f*1 for oxygen and cobalt atoms, correspondingly, was used for the solution of the Kohn-Sham equation. The exchange-correlated functional "Ceperley Alder" as a local density approximation was used for the electron-electron interaction [2]. Norm-conserving Troullier Martins pseudopotentials [3] were employed to describe the interaction between core and valence electrons.

Figure 1. Small pure Co-NP

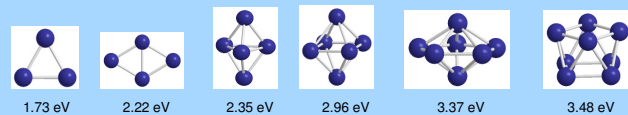


Figure 2. Chitosan molecule

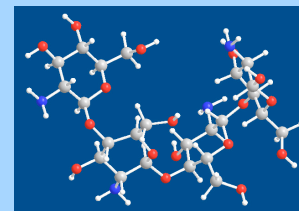


Figure 3. Increasing number of monomers of the chitosan molecule joined with Co<sub>7</sub>

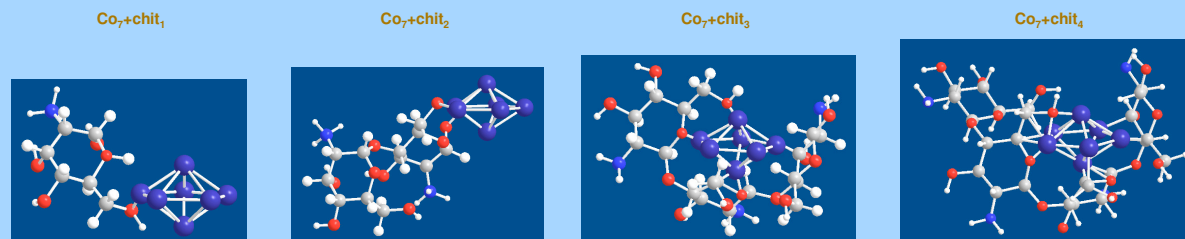


Figure 4. Total energy of the system Co<sub>N</sub>+chit<sub>N</sub> vs. the number of Cobalt atoms

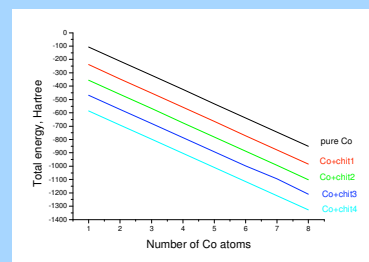
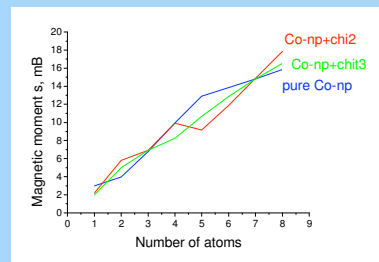


Figure 5. Magnetic moment of the system Co<sub>N</sub>+chit<sub>N</sub> vs. the number of Cobalt atoms



## Results

Stable structures of bare Co<sub>N</sub> ( $2 < N < 8$ ) clusters have been defined by global optimization of total energy. The most stable isomers are triangle, rhombus, trigonal bipyramid, tetragonal bipyramid, pentagonal bipyramid and tetragonal antiprism for 3-, 4-, 5-, 6-, 7- and 8-atomic clusters (Fig. 1). Magnetic moments of pure small stable Co-NP rise monotonously with increasing size of Co-NP. We have calculated how the total energy of Co-NP changes with attaching 2-, 3-, and 4-monomers chitosan molecule (Fig. 2,3).

We also have investigated magnetic properties of cobalt clusters into chitosan molecules depending on the size of Co-NP (Fig. 5). As expected compared with experimental results, the magnetic moment increased with increasing Co-NP size. Chitosan molecules in such small structures did not decrease total magnetic moment with increasing the size of Co-NP.

## References

1. T. Ozaki, Phys. Rev. B. **67**, 155108, (2003).
2. J. P. Perdew, K. Burke, and M. Ernzerhof, Phys. Rev. Lett. **77**, 3865 (1996).
3. N. Troullier and J. L. Martine, Phys. Rev. B **43**, 1993 (1991).

## Acknowledgements

This work was supported by DAAD Research Grant (Referat 326, 2009).

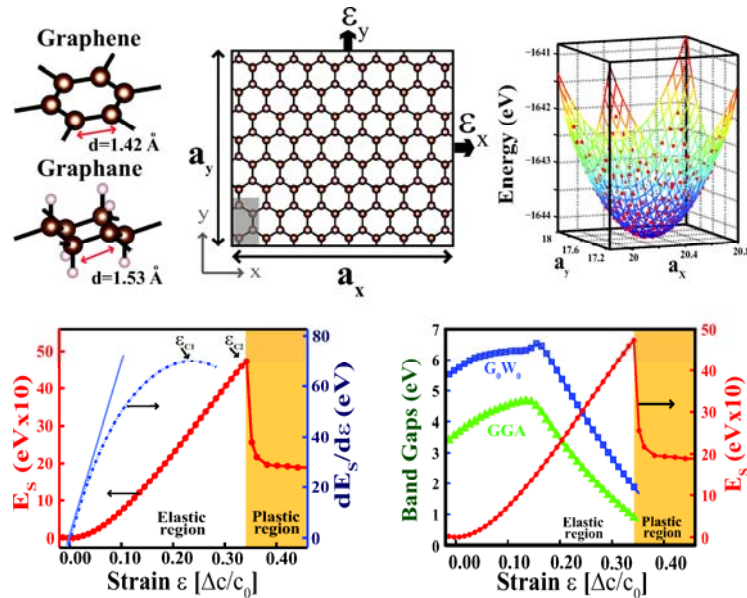
# The response of mechanical and electronic properties of graphane to the elastic strain

Mehmet Topsakal, Salim Çiracı

UNAM-Institute of Materials Science and Nanotechnology, Bilkent University, Ankara  
topsakal@unam.bilkent.edu.tr, ciraci@fen.bilkent.edu.tr

Two dimensional (2D) monolayer honeycomb structures of graphene[1] BN,[2] and silicon[3] offer remarkable properties and are promising materials for future applications. Honeycomb structure of graphene with  $sp^2$  bonding underlies the unusual mechanical properties providing very high in-plane strength. Graphene and its rolled up forms, carbon nanotubes are among the strongest and stiffest materials yet discovered in terms of tensile strength and elastic modulus.[4] Graphane, another member of honeycomb structures was theoretically predicted and recently synthesized by exposing graphene to hydrogen plasma discharge.[5] Here each carbon atom being bonded to one hydrogen atom is pulled out from the graphene plane and hence whole structure is buckled. Instead of being a semimetal like graphene, graphane is a wide band gap semiconductor and can attain permanent magnetic moment through hydrogen vacancies.

In this work, based on first-principles calculations, we revealed the elastic constants of recently synthesized monolayer hydrocarbon, graphane, using strain energy calculations in the harmonic elastic deformation range and compared them with those calculated for other honeycomb structures. The in-plane stiffness and Poisson's ratio values are found to be smaller than those of graphene. We also found that in the presence of hydrogen vacancy and carbon+hydrogen divacancy, its yielding occurs at smaller strains. Furthermore, its band gap first increases then decreases steadily with the increasing applied strain. We believe that our predictions are relevant for the current research focused on the electronic properties of honeycomb structures under strain.[6]



NOTE: This work is published as Applied Physics Letters **96**, 091912 (2010)

References:

- [1] K.S. Novoselov, et al., Science **306**, 666 (2004). [2] C. Jin, et al., Phys. Rev. Lett. **102**, 195505 (2009). [3] S. Cahangirov, et al., Phys. Rev. Lett. **102**, 236804 (2009). [4] C. Lee, et al., Science **321**, 385 (2008). [5] D. C. Elias, et al., Science **323**, 610 (2009). [6] M. Topsakal and S. Ciraci, Phys. Rev. B **81**, 024107 (2009) and the references therein.

# THE EFFECTS OF GEOMETRICAL PARAMETERS ON CARRIER STATES AND OPTICAL TRANSITIONS IN A QUANTUM RING

M. Triki<sup>a</sup>, D. Elmaghraoui<sup>a</sup> and S. Jaziri<sup>a,b</sup>

<sup>a</sup> Laboratoire de Physique de la Matière Condensée, Faculté des Sciences de Tunis, Tunisia.

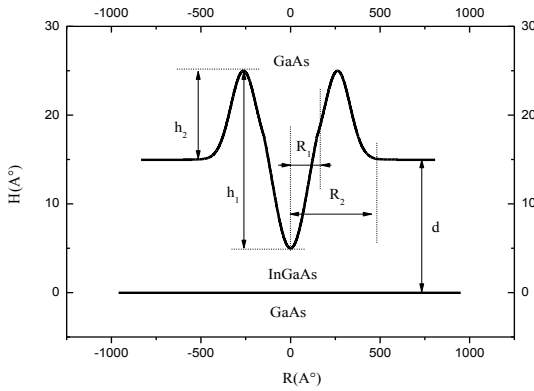
<sup>b</sup> Laboratoire de Physique et des Matériaux, Département de Physique, Bizerte, Tunisia.

## ABSTRACT

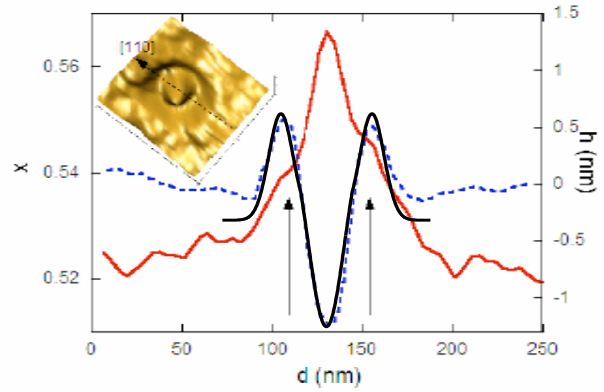
Using a numerical method via the electron effective mass theory, a model of QR with shape very close to the real one and taken from an experimental work, we investigate the electron states in semi-conductor quantum ring, studying the influence of the ring's geometrical parameters on the electron spectrum and on the optical transitions. Our hetero structure evolves from a single quantum dot to a quantum ring. We conclude that, unlike quantum dots, the ground state is with symmetry P which is energetically favored and our results are in good agreement with experimental data.

Keywords: Quantum ring; Electron spectrum.

## THEORITICAL MODEL:



Cross section of the quantum ring



Agreement of our model with an experimental one found by G. Biasiol et al [1]

The Schrödinger equation can be written as:

$$(H_0 + V)\psi(r) = E_{e,h}\psi(r) \quad \text{Where:}$$

$$V = V_{e,h}(1 - D(z, \rho))$$

$$H_0 = -\frac{\hbar^2}{2} \nabla \frac{1}{m_{e,h}(z, \rho)} \nabla$$

$$\psi(\rho, \theta, z) = \sum_{i,j} C_{i,j}^n \Phi_{i,j}^n(\rho, \theta, z)$$

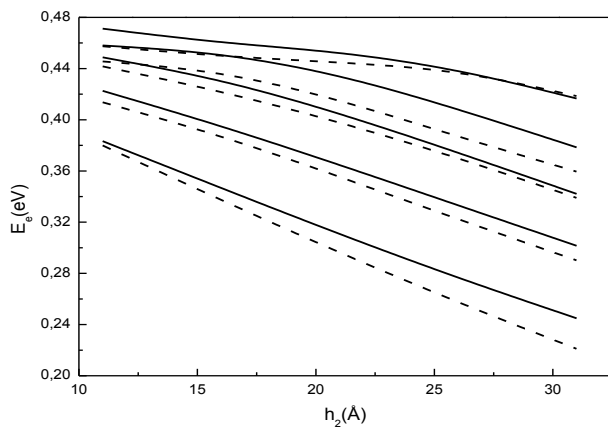
$$\Phi_{i,j}^n(\rho, \theta, z) = \alpha_i^n e^{in\theta} J_n \left( \frac{\lambda_i^n}{R} \rho \right) \sin\left(\frac{\Pi j z}{Z}\right)$$

Multiplying on the left by :  $\Phi_{i',j'}^{n'}^*$  Then integrating , yields the matrix equation :

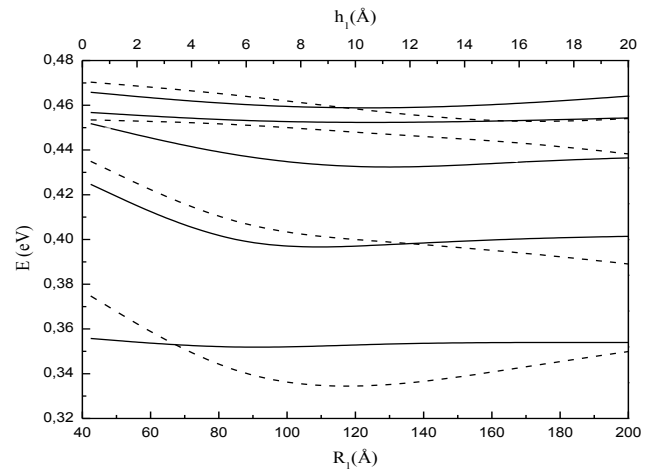
$$(A_{nij'n'j'} - E \delta_{n,n'} \delta_{i,i'} \delta_{j,j'}) C_{i,j}^n = 0$$

$$\begin{aligned} \text{Where:} \quad A_{nij'n'j'} &= \frac{\hbar^2}{2m_{GaAs}} \left\{ \left(\frac{\Pi j}{Z}\right)^2 + \left(\frac{\lambda_i^n}{R}\right)^2 + V_{e,h} \right\} \delta_{n,n'} \delta_{i,i'} \delta_{j,j'} \\ &+ \frac{\hbar^2}{2} \left( \frac{1}{m_{GaAs}} - \frac{1}{m_{In_xGa_{(1-x)As}}} \right) \int_{QR} (\nabla \Phi_{i',j'}^{n'}) (\nabla \Phi_{i,j}^n) \rho d\rho d\theta dz \\ &- \int_{QR} \Phi_{i',j'}^{n'} \Phi_{i,j}^n \rho d\rho d\theta dz \end{aligned}$$

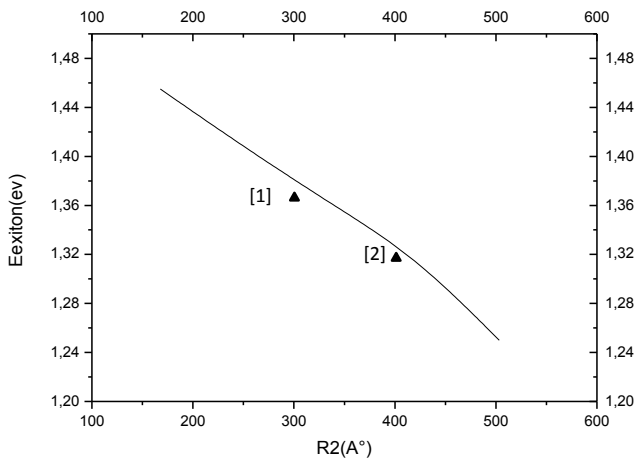
## RESULTS AND DISCUSSION



The electron spectrum as a function of the ring height



The electron spectrum of the ring as a function as the inner radius  $R_1$  and the crater height  $h_1$ .



Optical transitions as a function of the outer radius  $R_2$



- Energy levels decrease with the increase of  $h_2$
- The states with the symmetry P fall under those with the symmetry S
- Calculated optical transitions are very close to the experiment ones given by [1] and [2].

## CONCLUSION

- Based on the effective-mass envelope function theory, the electron band structure and the optical transition are calculated by using a numerical method.
- In our approach, we use a real shape for the QR.
- Our model can be adopted in calculating the electron or hole states of low-dimensional structures with arbitrary shapes.
- The results clearly show that the energy levels in the quantum ring change dramatically with the increase of its radius and its height. In particular we found that the first is with the symmetry P.
- Comparing our results to experimental ones, we have found that they are very close.
- We hope that our results will be helpful for studying and fabricating optoelectronic devices.

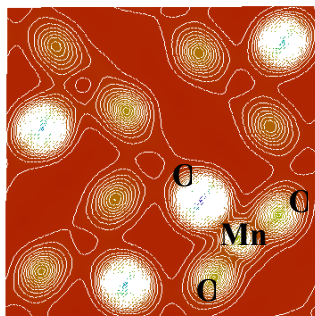
[1] G. Biasiol, R. Magri, S. Heun, A. Locatelli, T. O. Mentis, L. Sorba, J. Crystal Growth 311, 1764 (2009).  
 [2] D. Granados and J. M. Garcia App. Phys. Lett. 82, 2401 (2003).

# Magnetic and Opto-electronic Properties of Mn-doped Indium Tin Oxide

Madhvendra Nath Tripathi, Hiroshi Mizuseki, Yoshiyuki Kawazoe

*Institute for Materials Research (IMR), Tohoku University, Sendai 980-8577, Japan.  
Tel: +81-22-215-2054, E-mail address: ommadhav@imr.edu, ommadhav27@gmail.com*

The indium tin-oxide (ITO) has been widely investigated due to its excellent electrical and optical properties. It is one of the most widely used as transparent conducting materials in various optoelectronic devices. At present, major component of ITO is indium which is expensive and scarce so it is required to develop material with reduced amount of it. Recently<sup>1-4</sup>, it is reported that low doping of Mn ions in ITO films provides remarkable magnetic property without significant degradation in optical transparency. The electronic, optical and magnetic properties of manganese doped indium tin oxide (ITO) were calculated by using the density functional theory (DFT). Our spin polarized calculations show that the system is in magnetic ground state.



Charge density plot for Mn-doped oxidized Indium tin oxide (ITO)

## References:

1. Toshihiro Nakamura, Kohei Tanabe, Kazuki Tsureishi, and Kunihide Tachibana, *J. of Appl. Phys.* **101** (2007) 09H105.
2. M. Venkatesan, R. D. Gunning, P. Stamenov, and J. M. D. Coey, *J. of Appl. Phys.* **103** (2008) 07D135.
3. Toshihiro Nakamura, Shinichi Iozaki, Kohei Tanabe, and Kunihide Tachibana, *J. of Appl. Phys.* **105** (2009) 07C511.
4. Susmita Kundu, Dipten Bhattacharya, Jiten Ghosh, Pintu Das, Prasanta K. Biswas, *Chemical Physics Letters* **469** (2009) 313.

## **Localized Electric Field Confinement in a Quantum Well**

Allan L. Alinea, Ronald S. Banzon, Cristine Villagonzalo  
Structure and Dynamics Group  
National Institute of Physics, University of the Philippines  
Diliman, Quezon City 1101, Philippines

### ***Abstract:***

Particle confinement in a quantum well in the presence of an external electric field is investigated in this work. The localized electric field is generated by two electrodes which encompasses the quantum well. Using the variational Monte Carlo method, we demonstrate that the probability of the particle being confined approaches a step function with increasing electric field relative to the quantum well width. An effective threshold ratio between the electric field strength and the quantum well width can therefore be defined that measures the degree of coupling between the quantum well and the electrodes.

## Electrostatically confined quantum rings in bilayer graphene

M. Zarenia<sup>1</sup>, J. M. Pereira Jr.<sup>2</sup>, F. M. Peeters<sup>1,2</sup>, and G. A. Farias<sup>2</sup>

<sup>1</sup>*Department of Physics, University of Antwerp, Groenenborgerlaan 171, B-2020 Antwerpen, Belgium*

<sup>2</sup>*Departamento de Física, Universidade Federal do Ceará, Fortaleza, Ceará, 60455-760, Brazil.*

We propose a new system where electron and hole states are electrostatically confined into a quantum ring in bilayer graphene. This proposal is based on the fact that in bilayer graphene a gap in the electronic spectrum can be created and modified by means of a gate voltage<sup>1</sup>. Our approach differs from previous graphene-based quantum rings, which were created by cutting a graphene layer in a ring-like shape. Previous approaches have the disadvantage of introducing disorder at the edges of the graphene-based structure which may greatly influence the performance, and complicate the theoretical analysis of the device.

These issues do not arise in our system, since in our proposed structure the bilayer graphene sheet is assumed to be defect-free and the confinement is brought about by an external bias. That also means that the ring parameters can be tuned by external fields. Our results also display interesting new behaviors in the presence of a perpendicular magnetic field ( $B_0$ ), which have no analogue either in semiconductor-based or in lithography-based graphene quantum rings<sup>2,3</sup>, such as an overlap between magnetically confined Landau states (in which the carriers are mainly located in the center of the ring) and electrostatically confined states. In particular, the eigenvalues are not invariant under a  $B_0 \rightarrow -B_0$  transformation and, for a fixed total angular momentum index  $m$ , their field dependence is not parabolic, but displays two minima separated by a saddle point. The spectra also display several anti-crossings, which arise due to the overlap of gate-confined and magnetically-confined states. The existence of Aharonov-Bohm<sup>4</sup> oscillations for both electrons and holes are still linked with flux quantization through the ring. This novel spectra obtained for a finite width quantum ring<sup>5</sup> can be understood by means of a toy model for an ideal zero width ring in which case analytical results can be obtained<sup>6</sup>.

---

<sup>1</sup> J. M. Pereira Jr., P. Vasilopoulos, and F. M. Peeters, *Nano Lett.* **7**, 946, (2007).

<sup>2</sup> S. Russo, J. B. Oostinga, D. Wehenkel, H. B. Heersche, S. S. Sobhani, L. M. K. Vandersypen, and A. F. Morpurgo, *Phys. Rev. B* **77**, 085413 (2008).

<sup>3</sup> D. A. Bahamon, A. L. C. Pereira, and P. A. Schulz, *Phys. Rev. B* **79**, 125414 (2009).

<sup>4</sup> Y. Aharonov and D. Bohm, *Phys. Rev.* **115**, 485 (1959).

<sup>5</sup> M. Zarenia, J. M. Pereira Jr., F. M. Peeters, and G. A. Farias, *Nano Lett.* **9**, 4088, (2009).

<sup>6</sup> M. Zarenia, A. Chaves, J. M. Pereira Jr., F. M. Peeters, and G. A. Farias, *Phys. Rev. B* **81**, 045431 (2010).

## Thermodynamic and kinetic aspects of the breakage of a molecular nanowire. Effects of the metal and the linker group.

Martin E. Zoloff Michoff and Ezequiel P. M. Leiva  
Departamento de Matemática y Física  
Facultad de Ciencias Químicas  
Universidad Nacional de Córdoba  
Córdoba – Argentina  
*e-mail*: martinz@fcq.unc.edu.ar

The possibility of building ultra small electronic devices using single molecules has triggered numerous experimental as well as theoretical studies in the last few years.<sup>1</sup> Molecules are attractive building blocks since it is possible to tailor the properties of the contact modifying the nature of the anchoring group and also by introducing substituents on the molecule.

The 1,4-disubstituted benzene system, illustrated in Fig. 1, has been successfully used to build nanojunctions consisting of single molecules sandwiched between two metallic electrodes. Different anchoring groups have been used, such as cyanide (-CN), isocyanide (-NC) and thiol (-S), finding that the last two provide the strongest binding to the metal and that the conductance of these systems are similar with both Au and Pt electrodes.<sup>2</sup> On the other hand, the system with the cyanide linker does not show a distinct conductance. The amine (-NH<sub>2</sub>) linker has also shown reproducible conductance values that were attributed to a single molecule contact.<sup>3</sup>

Most of the theoretical studies performed on this type of system deal with conductance calculations. In this work we present a systematic study in which we evaluate the thermodynamic and kinetic stability of the nanojunctions formed between 1,4-disubstituted benzenes with varying anchoring groups (A = -S, -NC, -CN, -NH<sub>2</sub>, PCH<sub>3</sub>, -NCS, -COO) with Au and Pt electrodes. DFT calculations were performed with the SIESTA code to yield the bonding energy and the rupture force of the nanojunction. The Nudged Elastic Band (NEB) method was used to calculate the velocity of rupture as a function of an external pulling force.

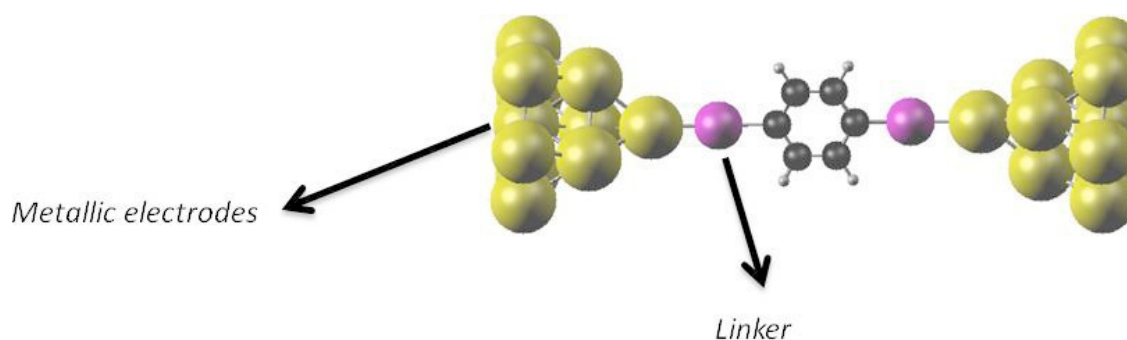


Fig. 1: Scheme illustrating the system studied. The linker is a functional group through which the molecules attaches to the metallic electrodes (see text).

1. Tao, N. J. *Nat Nano* **2006**, 1 (3), 173-181.

2. a) Kiguchi, M.; Miura, S.; Hara, K.; Sawamura, M.; Murakoshi, K. *Applied Physics Letters* **2006**, 89 (21), 213104-3. b) Kiguchi, M.; Miura, S.; Hara, K.; Sawamura, M.; Murakoshi, K. *Applied Physics Letters* **2007**, 91 (5), 053110-053113.

3. a) Venkataraman, L.; Klare, J. E.; Nuckolls, C.; Hybertsen, M. S.; Steigerwald, M. L. *Nature* **2006**, 442 (7105), 904-907. b) Quek, S. Y.; Venkataraman, L.; Choi, H. J.; Louie, S. G.; Hybertsen, M. S.; Neaton, J. B. *Nano Lett.* **2007**, 7 (11), 3477-3482. c) Quinn, J. R.; Foss, F. W.; Venkataraman, L.; Hybertsen, M. S.; Breslow, R. *J. Am. Chem. Soc.* **2007**, 129 (21), 6714-6715